



**NAVAL
POSTGRADUATE
SCHOOL**

MONTEREY, CALIFORNIA

THESIS

**MODELING ATMOSPHERIC EFFECTS ON WIRELESS
NETWORKS**

by

Amy Bleidorn

March 2008

Thesis Advisor:
Second Reader:

Karl Pfeiffer
Kenneth Davidson

Approved for public release; distribution is unlimited

THIS PAGE INTENTIONALLY LEFT BLANK

REPORT DOCUMENTATION PAGE			Form Approved OMB No. 0704-0188	
Public reporting burden for this collection of information is estimated to average 1 hour per response, including the time for reviewing instruction, searching existing data sources, gathering and maintaining the data needed, and completing and reviewing the collection of information. Send comments regarding this burden estimate or any other aspect of this collection of information, including suggestions for reducing this burden, to Washington headquarters Services, Directorate for Information Operations and Reports, 1215 Jefferson Davis Highway, Suite 1204, Arlington, VA 22202-4302, and to the Office of Management and Budget, Paperwork Reduction Project (0704-0188) Washington DC 20503.				
1. AGENCY USE ONLY (Leave blank)		2. REPORT DATE March 2008	3. REPORT TYPE AND DATES COVERED Master's Thesis	
4. TITLE AND SUBTITLE Modeling Atmospheric Effects on Wireless Networks			5. FUNDING NUMBERS	
6. AUTHOR(S) Amy Bleidorn				
7. PERFORMING ORGANIZATION NAME(S) AND ADDRESS(ES) Naval Postgraduate School Monterey, CA 93943-5000			8. PERFORMING ORGANIZATION REPORT NUMBER	
9. SPONSORING /MONITORING AGENCY NAME(S) AND ADDRESS(ES) N/A			10. SPONSORING/MONITORING AGENCY REPORT NUMBER	
11. SUPPLEMENTARY NOTES The views expressed in this thesis are those of the author and do not reflect the official policy or position of the Department of Defense or the U.S. Government.				
12a. DISTRIBUTION / AVAILABILITY STATEMENT Approved for public release; distribution is unlimited			12b. DISTRIBUTION CODE	
13. ABSTRACT (maximum 200 words) Wireless communications infrastructures can extend command and control rapidly across the battle space. This study analyzed signal propagation measurements from an 802.16 link in comparison to effects-based model output. The atmospheric data included in situ measurements, numerical weather model data, and standard profiles routinely used by operators. The network studied was located in a region of highly variable terrain and vegetation in Northern Thailand during the COASTS 2007 field experiments. Received signal data showed a weak correlation with predicted values using Advanced Refractive Effects Prediction System (AREPS) with in situ and model weather data. Additional comparisons with Interactive Scenario Builder (<i>Builder</i>) did now show similar performance as a tactical decision aid using variable propagation conditions.				
14. SUBJECT TERMS wireless networks propagation radiosondes AREPS Builder COASTS 802.16 WiMax models COAMPS			15. NUMBER OF PAGES 79	
			16. PRICE CODE	
17. SECURITY CLASSIFICATION OF REPORT Unclassified	18. SECURITY CLASSIFICATION OF THIS PAGE Unclassified	19. SECURITY CLASSIFICATION OF ABSTRACT Unclassified	20. LIMITATION OF ABSTRACT UU	

Standard Form 298 (Rev. 8-98)
Prescribed by ANSI Std. Z39.18

THIS PAGE INTENTIONALLY LEFT BLANK

Approved for public release; distribution is unlimited

MODELING ATMOSPHERIC EFFECTS ON WIRELESS NETWORKS

Amy L. Bleidorn
Lieutenant Commander, United States Navy
B.S., United States Naval Academy, 1998

Submitted in partial fulfillment of the
requirements for the degree of

**MASTER OF SCIENCE IN METEOROLOGY AND PHYSICAL
OCEANOGRAPHY**

from the

**NAVAL POSTGRADUATE SCHOOL
March 2008**

Author: LCDR Amy Bleidorn

Approved by: Lt Col Karl Pfeiffer
Thesis Advisor

Dr. Kenneth Davidson
Second Reader

Dr. Philip Durkee
Chairman, Department of Meteorology

THIS PAGE INTENTIONALLY LEFT BLANK

ABSTRACT

Wireless communications infrastructures can extend command and control rapidly across the battle space. This study analyzed signal propagation measurements from an 802.16 link in comparison to effects-based model output. The atmospheric data included in situ measurements, numerical weather model data, and standard profiles routinely used by operators. The network studied was located in a region of highly variable terrain and vegetation in Northern Thailand during the COASTS 2007 field experiments. Received signal data showed a weak correlation with predicted values using Advanced Refractive Effects Prediction System (AREPS) with in situ and model weather data. Additional comparisons with Interactive Scenario Builder (*Builder*) did not show similar performance as a tactical decision aid using variable propagation conditions.

THIS PAGE INTENTIONALLY LEFT BLANK

TABLE OF CONTENTS

I.	INTRODUCTION.....	1
A.	OVERVIEW	1
B.	OBJECTIVES.....	1
C.	RESEARCH QUESTIONS	2
D.	SCOPE.....	2
E.	ORGANIZATION OF THESIS.....	3
II.	BACKGROUND.....	5
A.	COASTS	5
B.	THAILAND CLIMATOLOGY.....	6
C.	WIRELESS SYSTEMS.....	7
1.	IEEE 802.11.....	7
2.	IEEE 802.16.....	8
D.	REFRACTION AND PROPAGATION.....	9
1.	Index of Refraction and Modified Refractive Index.....	9
2.	Trapping Layers and Ducting	13
3.	Propagation Loss	14
4.	Other Meteorological Effects on Signals.....	14
E.	ATMOSPHERIC PROPAGATION EFFECTS MODELS.....	16
1.	Advanced Propagation Model (APM).....	16
2.	AREPS	17
3.	<i>Builder</i>	18
III.	DATA COLLECTION AND PROCESSING	21
A.	EXPERIMENTAL DESIGN.....	21
1.	Network Set-Up and Monitoring	22
a.	<i>Thailand Back-haul Topology</i>	22
b.	<i>Network Monitoring Equipment</i>	23
2.	Meteorological Instruments and Models	25
a.	<i>Mini Rawinsonde System and RS-80 Radiosonde</i> ...	25
b.	<i>Coupled Ocean/Atmosphere Mesoscale Prediction System (COAMPS)</i>	26
3.	Propagation Model Set-Up and Input.....	27
B.	DATA PROCESSING.....	28
IV.	COASTS 2007 ANALYSIS RESULTS	31
A.	PROPAGATION EFFECTS	31
1.	Propagation Conditions	31
a.	<i>Atmospheric Profiles</i>	31
b.	<i>K-factor Calculations</i>	32
2.	APM Results in a Standard Atmosphere	35
3.	TDA Results vs Observed Propagation Loss Results.....	38
a.	<i>Trends in RF Data</i>	38
b.	<i>Hourly Received RF vs APM Predicted Power</i>	42

B.	ATMOSPHERIC AND EFFECTS BASED MODELS IN ISR PLANNING.....	43
1.	AREPS and <i>Builder</i> Comparisons.....	43
V.	SUMMARY.....	47
A.	DISCUSSION.....	47
B.	FUTURE RESEARCH.....	49
	LIST OF REFERENCES.....	51
	APPENDIX A - INPUTS TO PROPAGATION MODELS.....	55
	APPENDIX B – SNR/POWER CONVERSIONS.....	57
	APPENDIX C – CAAPS SUPPORT REQUEST.....	59
	INITIAL DISTRIBUTION LIST.....	63

LIST OF FIGURES

Figure 1.	M profile showing resultant trapping layer and duct.	13
Figure 2.	Advanced Propagation Model hybridization. (From Remcom 2003.).	17
Figure 3.	Relay link of 802.16 equipment from Mae Ngat dam.....	23
Figure 4.	RFMonitor plot showing changes in RSSI and SENADR with time. ...	24
Figure 5.	The Solarwinds chart shows available network monitoring parameters.	25
Figure 6.	Atmospheric profiles March 23-27 2007, as measured by RS-80 and predicted by COAMPS. The COAMPS in March was set for a position 20 km away from the balloon launch site (18.78N, 98.98E) which is evident in the starting altitude difference.	31
Figure 7.	Atmospheric profiles May 28-30 2007, as measured by RS-80 and predicted by COAMPS.	32
Figure 8.	K factors calculated for dz=100m and dz-1000m for each COAMPS and radiosonde profile. Large anomalies are seen at dz=100m.	33
Figure 9.	K factors calculated for dz-1000m for each COAMPS and radiosonde profile. Seasonal and diurnal variations are more evident at dz=1000m.	34
Figure 10.	For a standard atmosphere running APM, <i>Builder</i> and AREPS dBW at various ranges. The largest difference at 1400 feet may be due to terrain.	36
Figure 11.	AREPS outputs for 30 May 0800 at ranges of 2-10nm from the radio source at Mae Ngat. Environments used were COAMPS analysis for 30 May 0800 and in-situ Radiosonde launch at 30 May 0800. The largest loss difference is 3 dBW at a distance of around 4-6nm.	37
Figure 12.	Terrain heights from Mae Ngat radio site, showing ridge from 4-6 nm.	38
Figure 13.	Received power signals recorded from Solarwinds (Mae Ngat) and RFMonitor (METG) radios on 28 May 2007.....	39
Figure 14.	Hourly means plotted for each day of Received signal measurements. The (R) indicates Redline RSSI, with a correction factor added to bring to the same scale as Motorola rx power. The highest signals were often seen in the mid-afternoon.....	40
Figure 15.	Hourly means plotted, averaged over every day of received signal measurements. The period of 1000-1300 showed below average signal strength.	41
Figure 16.	Plot of AREPS predicted receive power based on COAMPS and radiosonde profiles, and measured signal from the Motorola 600 with Solarwinds.	42
Figure 17.	<i>Builder</i> diagram showing terrain. View is from METG tower looking back.....	45

THIS PAGE INTENTIONALLY LEFT BLANK

LIST OF TABLES

Table 1.	Available rawinsonde measurements in THA.....	26
Table 2.	K-factors calculated for radiosonde profiles and corresponding COAMPS profiles. Points used for the calculation were 100m and 1000m above ground level.	33
Table 3.	For various k-factors, <i>Builder</i> output for signal strength at varying vertical resolutions, or “steps” for the maximum, minimum, and standard k-factor. The vertical resolution affected the signal more than the k-factor used.....	35
Table 4.	<i>Builder</i> Communications project, antenna and emissions initial inputs.....	55
Table 5.	AREPS Communications project, frequency and display initial inputs.....	56

THIS PAGE INTENTIONALLY LEFT BLANK

ACKNOWLEDGMENTS

I would like to express gratitude to the following people:

- My husband, John, for his support, perspective, and sense of humor.
- My section-mates for working as a team to make it through NPS.
- LtCol Karl Pfeiffer, Dr. Ken Davidson, Ms. Mary Jordan, Mr. Dick Lind, and Ms. Amalia Barrios for their time and expertise.
- SPAWAR San Diego and PMW-180 for travel and equipment funding.
- The COASTS 2007-2008 students, faculty, reservists, and contractors.

THIS PAGE INTENTIONALLY LEFT BLANK

I. INTRODUCTION

A. OVERVIEW

Wireless networks can be used to provide significant technological advantage to U.S. and coalition forces. Wireless technologies enable rapidly deployable surveillance and command and control systems to enhance situational awareness on the tactical, operational, and strategic level. The performance of wireless networks is dependent on numerous factors, including the atmospheric environment. As military and security operations employ these technologies more widely, it becomes more important to quantitatively measure and predict losses caused by the environment. Integration of atmospheric impacts to mission planning and network topology will provide the warfighter an asymmetric advantage by exploiting the current and future state of the environment. The operator running a propagation loss model in support of wireless communications should also understand the losses expected in the system.

Numerous studies of atmospheric effects on signal propagation have focused only on frequency bands, without explanation for other inherent factors that may affect network performance. Conversely, documented guidance for network engineers often glosses over environmental effects on the channels within which they operate.

B. OBJECTIVES

The objective of this thesis is to evaluate the atmosphere effects-based models' signal loss predictions as indicators of actual wireless network performance. Additionally, this study will outline challenges in modeling propagation losses for wireless networks. We compare model outputs of signal losses over various distances given atmospheric changes, and at a given location over numerous days. Specifically, data collected from 802.16 sites as part of the Cooperative Operations and Applied Science and Technology Studies

(COASTS) will be used to evaluate Advanced Refractive Effects Prediction System and Interactive Scenario Builder software.

C. RESEARCH QUESTIONS

This study attempted to answer several initial research questions. They were:

1. Can Operational Electromagnetic (EM) Propagation models be used to predict performance of wireless networks overland?
2. Can an average value of signal loss due to atmospheric effects be determined given standard operating ranges of wireless radios?
3. How can real-time propagation conditions be best accessed and used by forward deployed personnel?
4. How can the military Meteorology/Oceanography community best support littoral Intelligence, Surveillance, and Reconnaissance (ISR) missions?

D. SCOPE

Within this research, we conducted field experiments to collect concurrent atmospheric and network data, then used these data to make comparisons of effects-based propagation models with varying atmospheric input. We extend our results to examine the vulnerabilities of wireless networking from the environment, to include an analysis of the best tactical decision aid (TDA) to support network planning.

Research topics in support of this thesis will include network protocols and their limitations, as well as known atmospheric effects on wireless networks at 2.4 and 5.8 GHz. Data collection will include COAMPS, upper air soundings, and network signal strength. Finally, we will conduct an analysis of effect-based model outputs and observations.

E. ORGANIZATION OF THESIS

The remainder of this thesis is organized as follows:

CHAPTER II: This chapter will consist of an explanation of the experiment under which the data was gathered. Additionally, it will include a literature review to explain wireless networking systems, effects of atmospheric propagation, and an explanation of the effects-based models.

CHAPTER III: This chapter will discuss the experiment efforts conducted in support of this thesis, to include the data collection process and instruments used. It will include explanations of the network monitoring software as well as the upper air sounding equipment and COAMPS model.

CHAPTER IV: This chapter will present the experimental results and analysis with respect to our original research questions.

CHAPTER V: This chapter will present a comparison of the effects-based models and recommendations for their implementation by personnel planning hastily formed networks. It will also address areas for future research.

THIS PAGE INTENTIONALLY LEFT BLANK

II. BACKGROUND

A. COASTS

This research was conducted as part of the Cooperative Operations and Applied Science and Technology Studies (COASTS) 2007 project. COASTS is an international field experimentation program involving students and faculty from numerous academic disciplines. The COASTS concept is to test low cost, commercial off the shelf (COTS), technological systems in order to provide effective solutions for operations such as force protection, maritime interdiction, search and rescue, and border patrol. The backbone to the technology is a wireless communication networking system that can provide real-time interoperability between the advantaged and disadvantaged user. In 2007 COASTS students, faculty, and contractors worked with numerous countries throughout Southeast Asia to test and display the advantages of secure wireless solutions. Throughout the field experiments and demonstrations, COTS wireless networking provided a signal footprint that extended command and control from the commander, to the operation centers, to the soldier within the battle-space environment (COASTS 2007).

A previous COASTS project included a statistical study to determine a correlation between humidity and data throughput in a hastily formed wireless network (Miller 2006). The strongest correlation Miller found in his data was that 78% of observed relative humidity variation can be explained by differences in temperature. This high correlation is obvious to a meteorologist who understands that, by definition, relative humidity is a ratio of the amount of moisture present to the amount of moisture that saturated air would contain at a given temperature. The amount of moisture that saturated air would contain increases with temperature. Hence, relative humidity would be negatively correlated with temperature if the amount of water vapor pressure, the true measure of water vapor density, were constant. Miller also found a weak linear relationship between relative humidity and network throughput, though his

regression had an R-squared value of 38.3, indicating a large number of residuals. Miller did not extrapolate his findings to determine if there was a correlation with actual water vapor pressure. Extending this initial study, the 2007 COASTS Meteorology team conducted five field experiments in 2007, three in California and two in northern Thailand to determine if an atmospheric impact was present. Further, the study included analyses of the way to obtain the responsible atmosphere description, if there was an impact. The overall experiments and scenario centered on the establishment of a rapidly deployable wireless network for information sharing between the U.S. and its regional partners. The COASTS 2007 meteorology study focused on finding a correlation between atmospheric variables and the signal strength of the network backbone. This study focuses on the data gathered during the Thailand experiments in 2007, when atmosphere and surface data collection methods were the most robust in conjunction with these later field exercises.

B. THAILAND CLIMATOLOGY

The Thailand experiments were conducted in March and May 2007, around the time of the onset of the Southeast Asian Monsoon. A study of Thailand climatology (Higdon 2004) shows a trend that the country experiences very dry conditions from December through April. During this time, the Northeast Monsoon is in effect, and by the time air reaches Thailand it has lost most of its moisture. During these months, there is typically subsidence inversion. Also, as many farmers practice slash and burn, there is considerable haze and high aerosol content in the air, which was especially noticeable in the area of operations during the March testing.

From March to May, Thailand transitions to the southwest monsoon. The Asiatic low pulls in air, and the monsoon trough moves north over the country. There is typically increased convection and considerable moisture aloft. The convergence zone passes north, and the rain the systems bring washes out suspended aerosols. Fog dissipates early in the day as the stability of the air

column decreases. The southwest monsoon is in full effect from June through November. From November through the spring, the Asiatic low shifts to become the Asiatic high, and Thailand shifts back to the northeast monsoon.

C. WIRELESS SYSTEMS

The hardware tested in the field used two primary wireless protocols: the IEEE 802.11 and the IEEE 802.16. These standards operate in the 2.4 GHz and 5.8 GHz bands.

1. IEEE 802.11

Wireless communications require standardization in order to be widely compatible. The Institute of Electrical and Electronic Engineers maintains the international “standards” for technologies using radio frequencies. The 802.11 standard allows wireless vendors to integrate products. The importance in the protocol is that wireless networks are not sending a constant signal on a single frequency. A wireless local area network (LAN) can use either frequency hopping or a direct sequence and may not always be at an exact frequency such as 5.800 GHz as suggested above (Alexander 2005).

Just as the 802.11 protocol is not on a single frequency, it is also not a constant signal with time. The range of the wireless signal is not only a function of power. (Alexander 2005). Modems are able to compress large amounts of data onto a given bandwidth. However, as data is compressed it requires a cleaner and stronger signal to be understood on the other end. As distance increases between the signal and the receiver, it is harder to distinguish between signal and noise and the speed slows down, no matter how many watts of power are available. In general, the higher the data rate, the shorter the range.

A number of factors can cause transmission losses in a wireless network. (Alexander 2005) These can include the cabling and connectors used, and

obstructions such as walls causing absorption or reflection. In the next section we discuss the atmospheric effects. These are commonly accounted for as an approximate system loss in decibels.

2. IEEE 802.16

The 802.16 protocol expanded on the capabilities of 802.11, but with added security and increased ranges. It is also known as the Worldwide Interoperability for Microwave Access (WiMAX). The increased range adds challenges to 802.16 design, in that the range of interference typically exceeds the operating range (Cooklev 2004). 802.16 is designed for various frequency bands, but 2.4 and 5.8 GHz are used because of FCC imposed restrictions (Alexander 2005). In these unlicensed frequencies, power output is limited and other users can cause interference. Multipath in the 2-11 GHz range can be significant, and the antenna and receiver may not be in line of sight. Certain modulation schemes can handle reflection better.

An important part of 802.16 equipment is its improved ability to allow multiple access. This is done through a variety of duplexing schemes to allow concurrent uplink and downlink transmissions. When an 802.16 subscriber substation is linking to a base station for the first time, the stations exchange a ranging message, which helps to determine power adjustments, frequency adjustments, and timing offsets for optimal communication. The stations periodically update these health statistics during their routine exchanges (Cooklev 2004). Improvements to the current standard, IEEE.16-2004, add a standard for mobile capability as well as mesh networking capabilities, allowing each radio to communicate point-to-point with any other in the network.

Two of the major improvements from 802.11 that are realized in the 802.16 standard are increased layers of security and increased bandwidth efficiency. The increased efficiency is a result of Orthogonal Frequency Division Multiplexing (OFDM) and Time Division Duplexing (TDD). OFDM, by using multiple frequencies, allows more data to be carried than was previously possible

on the given frequency bandwidth. The OFDM waveform is also resistant to interference, because even if one of the sub-carriers of the OFDM waveform is disrupted, the others can maintain a partial link. This is useful where radio-frequency (RF) multi-path is an issue, such as around vegetation or a rough sea-surface. The advantage of the TDD multiplexing is that the system schedules a specific time for each subscriber to transmit data. This ensures any data packet transmitted on the network is received in a timely manner. (IEEE 2004)

D. REFRACTION AND PROPAGATION

Atmospheric impacts on propagation can include gaseous and particulate absorption of energy, or molecular refraction, which alters the wavefront's orientation and causes convergence or divergence of RF energy. Refraction can cause either beyond line-of-sight or less than line-of-sight reception ranges. The frequencies involved in the network field tests were too low to consider absorption as a serious cause for atmosphere impact (Myers 1999 and Rinehart 1991). Temperature and humidity can change horizontally and vertically in the atmosphere. Vertical temperature and humidity gradients, together with buoyancy effects and wind mixing, can cause variation of RF propagation conditions over shorter (longer) periods of time and smaller (larger) areas than usual. These changes affect refraction and, hence, wave propagation through varying refraction gradients.

1. Index of Refraction and Modified Refractive Index

Refraction is the bending or tilting of a wave-front as it propagates through a medium with spatially varying characteristics. The radio refractive index N valid for frequencies 100 MHz to 80 GHz is given in terms of temperature (T) in K, vapor pressure (e) in hPa, and total atmospheric pressure (P) in hPa.

$$N = 77.6 \frac{P}{T} + 3.73 \times 10^5 \left(\frac{e}{T^2} \right) \quad (1)$$

(Bean and Dutton, 1966 and ITU-R P453-7)

The vertical gradient of N describes the ray geometry of the EM wave. The expression for this gradient, dN/dz may be formed from the chain rule:

$$\frac{dN}{dz} = \frac{\partial N}{\partial P} \frac{dP}{dz} + \frac{\partial N}{\partial T} \frac{dT}{dz} + \frac{\partial N}{\partial e} \frac{de}{dz} \quad (2)$$

Partial differentiation of Equation 1 yields expressions for the partial N terms, and equation 2 can be rewritten as:

$$\frac{dN}{dz} = C_1 \frac{dP}{dz} + C_2 \frac{dT}{dz} + C_3 \frac{de}{dz} \quad (3)$$

Using Equation (3), dN/dz can be calculated from the vertical gradients of P, T, and e as measured by a radiosonde or as estimated by a value such as a standard atmosphere. Using representative conditions:

$$P = 1013 \text{ mb} \quad dP/dz = -120 \text{ mb}$$

$$T = 288 \text{ K (15 C)} \quad dT/dz = -6.5 \text{ K/km}$$

$$e_0 = 10 \text{ mb} \quad de/dz = -3.33 \text{ mb/km}$$

From (1):

$$\frac{\partial N}{\partial P} = \frac{77.6}{T} = \frac{77.6}{288} = .27(\text{mb}^{-1})$$

$$\frac{\partial N}{\partial T} = \left(-\frac{77.6}{T^2}\right)\left(P + 9613\left(\frac{e}{T}\right)\right) = \left(-\frac{77.6}{288^2}\right)\left(1013 + 9613\left(\frac{10}{288}\right)\right) = -1.27(\text{K}^{-1})$$

$$\frac{\partial N}{\partial e} = \frac{3.73 \cdot 10^5}{T^2} = \frac{3.73 \cdot 10^5}{288^2} = 4.50(\text{mb}^{-1})$$

Substituting into (2), dN/dz for near surface values becomes:

$$\frac{dN}{dz} (\text{km}^{-1}) = .27 \frac{dP}{dz} - 1.27 \frac{dT}{dz} + 4.5 \frac{de}{dz} \quad (4)$$

Wave fronts tilt in the atmosphere toward higher values of N. When dN/dz is positive (N increasing with height), waves are bent upward and away from the earth toward space. This is known as subrefraction. Subrefraction occurrence is

a factor in overland considerations, such as this, since it can occur when the sun heated surface becomes much warmer than the overlying air, in the absence of a humidity gradient.

When dN/dz is less than zero (N decreasing with height), normal refraction occurs and waves are bent down toward the earth's surface. A phenomenon called trapping occurs when dN/dz is less than -0.157m^{-1} . In this instance, refraction is so strong that EM waves bend toward the earth with a radius of curvature less than the earth's radius. Under certain conditions, the waves are reflected off the earth back into the lower atmosphere, and then refracted down again to the surface where the process continues, forming a wave-guide immediately above the surface.

A modified refractive index (M) was created to show the refractive ray relative to the earth's surface:

$$M = \frac{dN}{dz} + 0.157z \quad (5)$$

To simplify the above explanations, negative M gradients correspond to levels of trapping in the atmosphere. A positive gradient will show EM waves escaping the atmosphere, and a zero M gradient will show levels of neither trapping nor escaping (Battan 1973).

Another important parameter in radio meteorology is the k-factor. Also based off the refractive index N, the k-factor is a ratio between the effective earth radius for RF propagation and the actual earth radius. First, the radius of curvature of the ray can be calculated by

$$r_{ray} = \frac{n}{\left(\frac{dn}{dz}\right)} \quad (6)$$

This can be simplified with sufficient accuracy in N units as

$$r_{ray} = -\frac{10^6}{\left(\frac{dN}{dz}\right)} \quad (7)$$

The curvature of the ray is $1/r_{ray}$, while the curvature of the earth is $1/r_0$, or $1/6370$ km. In a coordinate system in which the ray is a straight line, the k factor in terms of equivalent radius of the earth, r_e , is

$$k = \frac{r_e}{r_0} = \left(\frac{1}{1 + \frac{r_0}{r_{ray}}} \right) = \frac{1}{1 - \frac{r_0}{10^6} \frac{dN}{dz}} \quad (8)$$

Equation 8 shows that positive gradients of N have lower k values, and negative have gradients have larger k values. Schelleng (1933) determined that in standard propagation conditions, a factor of 1.33 could be used as a “median” value. He based his calculations on values presented in Humprey’s (1929) the *Physics of Air* and it is not based on a seasonal, diurnal, or spatial variations. It is actually the average of summer and winter values, which he recognized as a factor at the time. The calculation was based on the gradients between 0 and 500m above sea level. This number has since been termed the k factor, or 4/3’s earth. This fictitious radius allows for easier calculations of other model parameters, as was necessary at the time of its inception. It does not use ray tracing, but only a slope between the refractivity of two points that are a distance, z, apart. Variations in atmospheric refractive conditions cause changes in the effective earth radius factor (k-factor) from its “median” value of 4/3 for the standard temperate atmosphere.

Considerations for radio placement in a wireless network includes clearing terrain and obstacles in the Fresnel zone. As stated in Rao et al. (1987) recommend a guideline of $k=1$ for wet climates and as low as $k=0.5$ for desert areas. Harvey (1987) lists “worst case” k-factors down to $k=0.39$ as measured in Australia.

When the earth is sufficiently subrefractive (that is, when k assumes low values), the rays will be bent in such a way that the earth appears to obstruct the direct path, giving rise to diffraction fading. Values of k exceeded 99.9% of the time are important for the determination of path clearance criteria.

2. Trapping Layers and Ducting

A duct is a wave-guide associated with a trapping layer that can result in extended ranges. The top of the trapping layer constitutes the top of the duct. This is where the value of the M gradient changes from negative to positive. If a duct exists, the bottom of the duct is the level at which an M value occurs equal to the trapping layer top minimum. It is possible to have more than one duct within a given atmospheric profile. At the upper boundary of the duct, rays that were directed upward turn downward relative to the earth's surface. At the duct's lower boundary, rays directed downward turn upward relative to the earth's surface. It follows that the ray curvature will be downward (relative to earth) where $dM/dz < 0$ and upward (relative to earth) where $dM/dz > 0$. Figure 1 depicts a standard ray trace example:

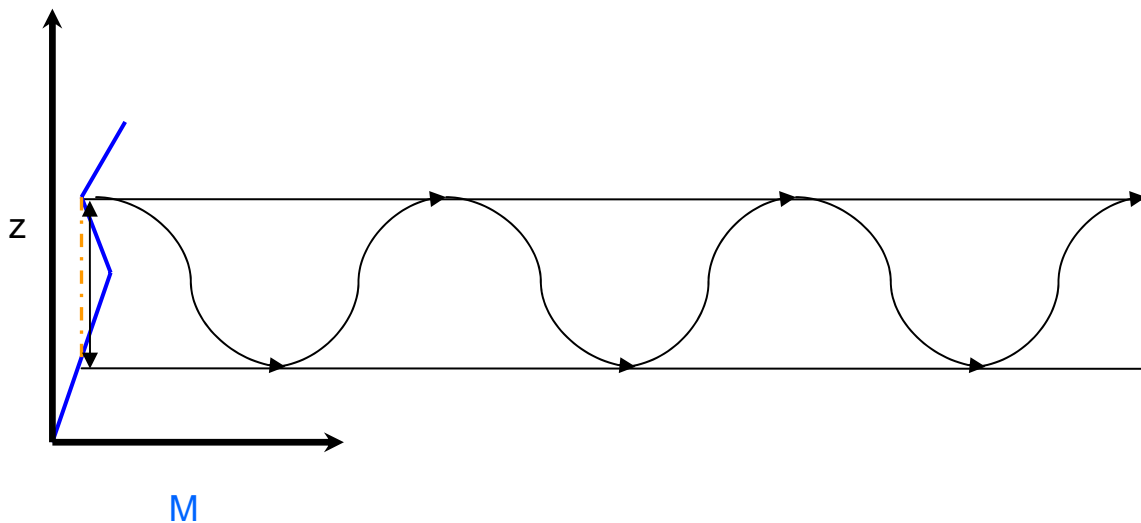


Figure 1. M profile showing resultant trapping layer and duct.

The transmitter must be located within the duct for complete energy channeling to occur. However, not all frequencies are trapped. An approximate empirical formula provides the relationship between the frequency, in Hz, that will be trapped given a certain duct height, d , in meters (m):

$$f_{\min} = \left(\frac{3.6 * 10^{11} \text{ Hz}}{m^{(-3/2)}} \right) * d^{(-3/2)} \quad (9)$$

(Davidson 2003)

Given formula (9), for a duct to exist at 5.8 GHz, it must be a depth of approximately 16 m, and at 2.4 GHz, it must be a depth of about 28 m.

Climatology shows that elevated trapping layers and associated ducts occur up to 16% of the days and nights in the winter months in the Chiang Mai area, and less often in the summer. This is based on statistics compiled by GTE Sylvania for use within AREPS.

3. Propagation Loss

Propagation loss is the amount of signal strength lost in an EM wave as it propagates away from its point of origin. Barrios (2003) used the following equation within the Advanced Propagation Model (APM):

$$L = 20 \log^* \left(\frac{4\pi r}{\lambda} \right) - 20 \log \left| \frac{E}{E_o} \right| \quad (10)$$

where L is propagation loss, r is range from the transmitter, λ is the wavelength, and $\left| \frac{E}{E_o} \right|$ is a propagation factor, which is normalized for isotropic antennas.

From this equation, it is evident that propagation loss increases with range and is inversely proportional to wavelength.

4. Other Meteorological Effects on Signals

There are numerous effects that temperature, precipitation, and particulates can have on networks. These are listed below as further

considerations in network modeling, but this study will be limited to primarily the effects of vertical atmospheric gradients on analogue signals.

- Rao et al. (1987) describe the effects of refractive environments on Fresnel zone clearance. Their research was conducted on microwave frequencies in India in March and shows the rays clear a specific hill given some refractive conditions, but often can not given subrefractive conditions.
- Hitney (1985) explains the effects of troposcatter at distances greater than line of sight, based on refractive index fluctuations, i.e., scintillation. He also describes the effects on propagation if lateral homogeneity is assumed but does not exist.
- Myers (1999) compares models for effects of rain attenuation on 802.16 signals, due to absorption and scattering, including effects of the polarization of the system on the attenuation. Based on this and previous studies specifically involving the physics of water droplets, attenuation due to moisture was not expected to be a factor at any frequency lower than 6 GHz, especially for the small size of particle which makes up water vapor and therefore humidity.
- Rinehart (1991) includes tables for attenuation at various rain rates and snow for specific wavelengths.
- The *Builder* Users manual (NRL 2003) describes one effect of temperatures on electronics. It states that the ambient temperature of the receiving device, (including the antenna, transmission line, and receiver) is used to calculate how much noise is created by the receiving systems themselves, independent from the external noise received through the antenna.
- Oraizi and Hosseinzadeh (2003) specifically addressed the effects of atmospheric ducts on OFDM broadcasting systems at various frequencies in sub-refractive, standard, and ducting conditions.
- Dodgett (1997) described the sensitivity of a propagation model around 3 GHz to the inputs of pressure, temperature and humidity.

E. ATMOSPHERIC PROPAGATION EFFECTS MODELS

Models that enter considerations of atmosphere effects on RF systems are propagation models, and effects models. Propagation models enable loss of energy at a given range to be influenced by atmosphere refraction. The Advanced Propagation Model (APM) is one of these. Effects models relate this loss to thresholds for detection of different targets and apply display tools to show the impact on missions. The Advanced Refractive Effects Prediction System (AREPS) and the Scenario Builder (*Builder*) are examples of Effects models. Both of these can use APM as the propagation model.

1. Advanced Propagation Model (APM)

The Advanced Propagation Model (APM) provides the propagation theory and calculations behind the AREPS and *Builder* tactical decision aids. APM is valid for the 100 MHz to 20 GHz frequency range. APM is an extension of previous model that was based solely on ray analyses. SPAWAR Systems Center (SSC) developed APM out of the necessity to incorporate several known limitation to ray analyses, including improved terrain-influenced EM model (Barrios 2003).

APM begins to calculate field strength for a region by use of the Parabolic Equation (PE) algorithm for propagation loss under a maximum propagation angle, which in turn dictates maximum ranges and heights. It then calculates propagation loss for other predetermined zones using three other algorithms shown in Figure 2. They are the flat earth (FE), the ray optics (RO), and the extended optics (XO) algorithms. The RO model is used for angles above the maximum PE propagation angle but less than 5 degrees elevation. The FE algorithm is applied for all heights and ranges out to 2.5 km from a source and elevation angles greater than 5 degrees. The XO model is then applied to areas above the PE region and outside the RO region.

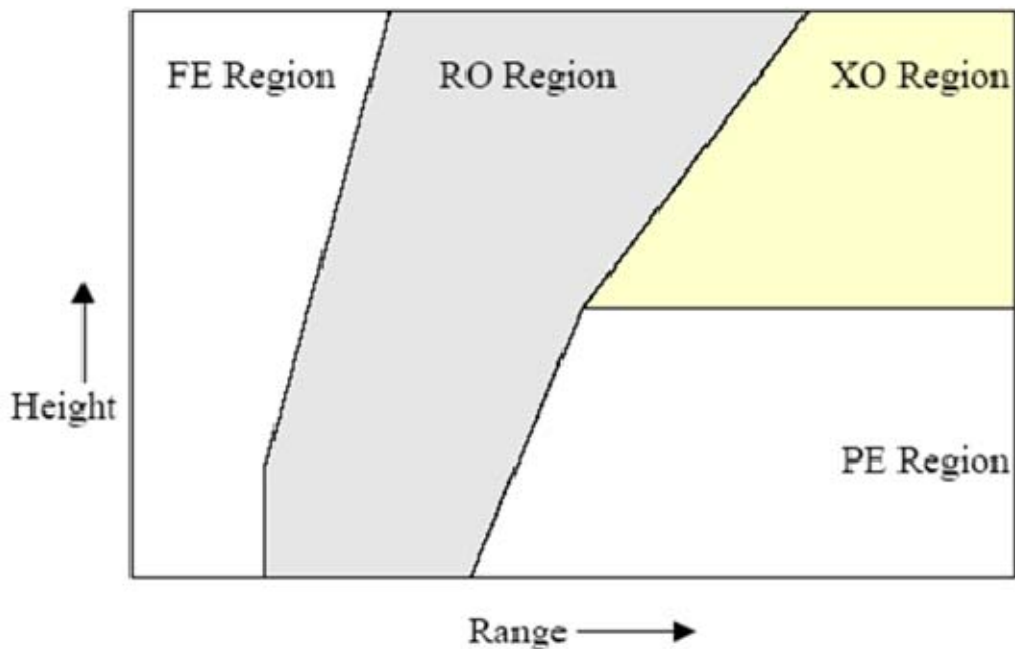


Figure 2. Advanced Propagation Model hybridization. (From Remcom 2003.)

Levy and Craig (1989) determined that application of the parabolic equation method used with radiosonde data is a powerful tool for the prediction of RF propagation. This was especially true at a high resolution, slow ascent rate, and the predictions were consistent even in the presence of noisy refractivity data.

2. AREPS

The Advanced Refractive Effects Prediction System (AREPS) is a propagation effects model developed by the Space and Naval Warfare Systems Center, San Diego (SPAWAR Systems Center, SSC). The sponsor for AREPS is primarily the Oceanographer of the Navy. The current program manager is PEO C4I PMW 180, MetOc Systems. AREPS is a Graphics User Interface (GUI), that incorporates environmental and communications system input with the Advanced Propagation Model (APM). The output is two-dimensional views of propagation

loss, vertical M-profiles, and propagation condition summaries based on model calculations. It uses either preloaded environments, such as a sample standard atmosphere, resample ducted atmospheres, or specific imported environments from rawinsonde data or models, such as COAMPS.

AREPS can use climatological, model derived, or directly measured atmospheric profiles. AREPS also has the capability to model different antenna types and frequencies. The AREPS software plots propagation loss values in color-coded graphs for visual interpretation by the user.

AREPS results are provided as one-way propagation loss. Specifically, the AREPS Users Manual (Atmospheric Propagation Branch SPAWAR 2006) defines propagation loss in the following way:

The ratio, expressed in decibels, of the effective radiated power transmitted in the direction of maximum radiation of the antenna pattern to the power received at any point by an omnidirectional antenna. In AREPS, propagation loss is equivalent to path loss when an omnidirectional antenna is specified... Therefore, propagation loss would be equal to transmission loss plus the antenna gain in decibels.

SPAWAR released AREPS version 3.6.02.79 on 26 February 2008. All analysis using AREPS is based on this version.

3. *Builder*

The Interactive Scenario Builder (*Builder*) is a three dimensional, Radio Frequency Tactical Decision Aid developed by the Naval Research Laboratory, code 5774, Washington D.C. The Office of Naval Research sponsored its development. The Naval Research Laboratory designed *Builder* to provide visualization of the RF capabilities of platforms in conjunction with geo-spatial situational awareness. It models communication and radar systems by calculating one-way and two-way RF propagation loss. It incorporates complex antenna pattern data as well as the effects of meteorology, terrain, and

environment when computing power level results (Remcom 2003). The user has the options of numerous propagation models, though we will only investigate APM in this study.

A difference between AREPS and the current version of *Builder*, is *Builder's* inability to input measured in-situ data into the METOC effects section. It does allow the user to input some meteorological measurements, but does not allow for uploading a radiosonde profile. Allowed environmental inputs include k-factor, surface based duct (elevated duct) height, surface duct height, surface humidity, surface wind speed, temperature, surface duct intensity, and surface based (elevated) duct intensity. When choosing the duct strength, the user can only be subjective, as the *Builder* options for duct strength are none, weak, average, strong, and extreme.

EMPIRE is the component of *Builder* that specifically models RF propagation. EMPIRE / *Builder* have the ability to incorporate real-time weather model data from the Fleet Numerical Meteorological and Oceanographic Center or the Air Force Weather Agency. For non-real time data, methods exist to build an atmospheric profile by creating a staging directory for the GRIB files and subsequently running a utility named "EMFProcessor," available at <https://builder.nrl.navy.mil>. The COAMPS GRIB fields required for this process are: Terrain height (surface), Surface roughness length (surface), Scale surface wind velocity (u^*) (surface), Scale surface temperature (t^*) (surface), Scale surface mixing ration (q^*) (surface), Wind speed, u-component (first sigma level), Wind speed, v-component (first sigma level), Pressure (3D volume), Temperature (3D volume), and Mixing Ratio (3D volume).

Empire computes a quantity termed "Transmission loss." This is the ratio of the power radiated by the transmitting antenna to the power available at the receiving antenna if there were no loss in radio frequency circuits. For a communications project, *Builder* provides results in terms of signal-to-noise ratio (SNR), or signal strength levels in dBW. Conversions between *Builder* and AREPS are shown in Appendix C. *Builder* version 3.13 Build 61102173 was used in this analysis.

THIS PAGE INTENTIONALLY LEFT BLANK

III. DATA COLLECTION AND PROCESSING

A. EXPERIMENTAL DESIGN

Our primary goal was to compare atmospheric conditions with either signal strength or network performance. A team of two NPS officer students collected data in the field in conjunction with the COASTS network team. NPS staff provided equipment and mesoscale prediction data.

The atmosphere data were selected based on requirements for validating electromagnetic (EM) propagation models' prediction of impacts on wireless networks. Based on previous experiments (Hitney 1985) and the preceding explanations, the primary atmospheric descriptor required was gradients of humidity and temperature with height, which affect RF propagation at high frequencies such as the microwave frequencies used in the COASTS scenario.

With regard to network transmission data, we wanted a measure of the signal strength or propagation loss of a wireless network, to compare to the output of the propagation models. Previous field experiments focused primarily on atmospheric impact on communication and radar frequencies, have applied various equipment to quantify the RF strength variations or network performance. Barrios (2006) used signal power received at an antenna for a VHF communication experiment. Miller (2006) used IX Chariot software to determine throughput of an 802.11 wireless network, while the VOCAR experiment used spectrum analyzers at the locations of each radio. (Paulus 1995).

Experiences and events in early COASTS field experiments enabled experimentation with approaches and compilation of ideas to determine how to best measure the impacted signal property of interest. Early in the process, we determined that although signal throughput was a good indicator of network performance, it could not be easily correlated to environmental changes. Throughput is highly susceptible to many other factors such as network traffic, number of components, and topology.

Based on these limitations, we decided to use software specifically designed for network engineers. The software enables engineers to monitor network data for analysis or problem diagnosis. These tools were Solarwinds Toolset and RFMonitor, described in a following section.

It was also necessary to determine from which radios we would collect data. The COASTS topology called for over 30 802.11 and 802.16 nodes in the Thailand demonstration. We chose the 802.16 backhaul nodes because they were permanently installed. This limited the number of variables that would be present when correlating received signal strength with measured meteorological changes. Additionally, these radios were at a distance far enough apart to prevent excessive signal bleed.

1. Network Set-Up and Monitoring

a. Thailand Back-haul Topology

For the COASTS 07 scenario at the Mae Ngat dam area of operations (AO), the team deployed 802.11 access points to create a wireless cloud over the dam area. This allowed for connectivity between the various cameras and sensors, which were set up in support of the maritime interdiction and search and rescue scenarios. 802.16 radios were set up to pass the information from the AO to a Royal Thai Air Force facility known as Wing 41. A series of five 802.16 radios made by two manufacturers were installed on cell towers in order to provide a “back-haul” to pass the information securely. The network topology of these radios is shown in Figure 3. The data travelled on a terrestrial line from Wing 41 to the Royal Thai Air Force headquarters in Bangkok, over 700 km away. The topology also included a redundant link to the IIFC tower for the information to be shared by the Interagency Intelligence Fusion Center.

Based on a site-survey, the team knew that the links between the METG, CHCM, IIFC, and WING 41 would be line of sight. The main concern was that the topology required a tower installation specifically for the radio at

Mae Ngat dam in order to provide the vertical clearance to link with MET-G. For this reason, Mae Ngat dam is the primary link of interest in this study.

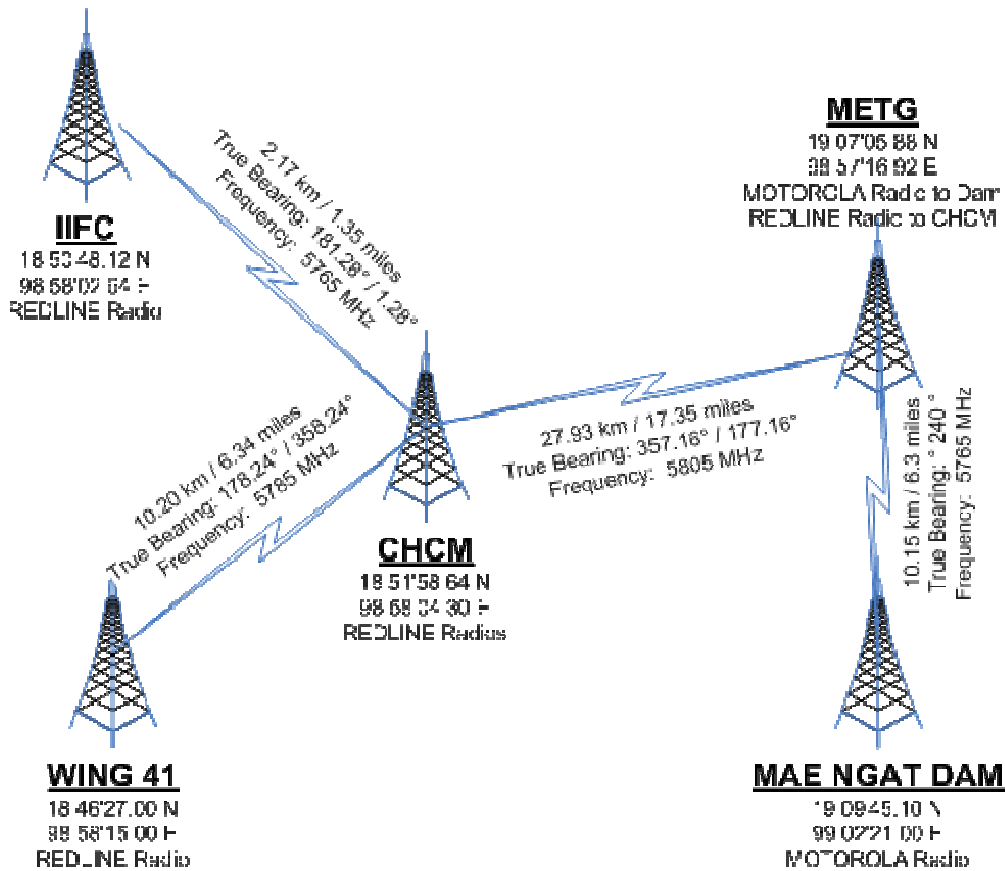


Figure 3. Relay link of 802.16 equipment from Mae Ngat dam

At each radio, flat panel directional antennas were used; their specifications as entered into the propagation models are listed in Appendix B.

b. Network Monitoring Equipment

The 802.16 radios selected for the testing and demonstration were the Redline AN-50E's and the Motorola PTP 600's. RFMonitor software measured the signal between Redline radios. The Redline company released this tool to automatically poll a web interface for current received power and signal to noise distortion ratio (SENADR) values. RF Monitor records this data

and provides plots and spreadsheets of the results at approximately one second intervals. An example of an RFMonitor chart is shown in Figure 4.

RFMonitor data are available for the Redline radio links between METG and CHCM, as shown in Figure 3 for the following dates: 22-23, and 26-27 March 2007, and 25, 28, and 29 May 2007.

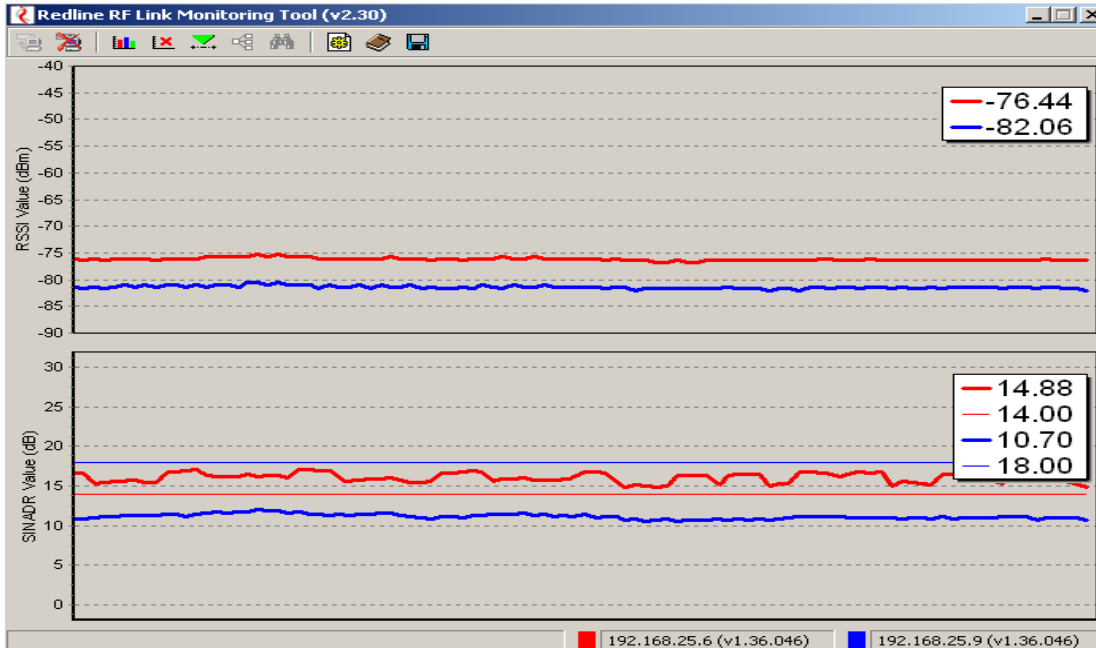


Figure 4. RFMonitor plot showing changes in RSSI and SENADR with time.

Between Motorola radios, we used *SolarWinds* v9.0 to record system parameters. *SolarWinds* plots data received directly from the Simple Network Management Protocol (SNMP) agent imbedded within the radios. This protocol is widely accepted as the preferred means of network management, and allows for remote monitoring and management of network systems. *Solarwinds* collected the following parameters of interest at varying intervals: Received Signal Strength, Signal to Noise Ratio (SNR), and Transmit power. *Solarwinds* data are available 27 March 2007, and 23- 25, 28-30 May 2007. An example of a *Solarwinds* chart is shown in Figure 5.

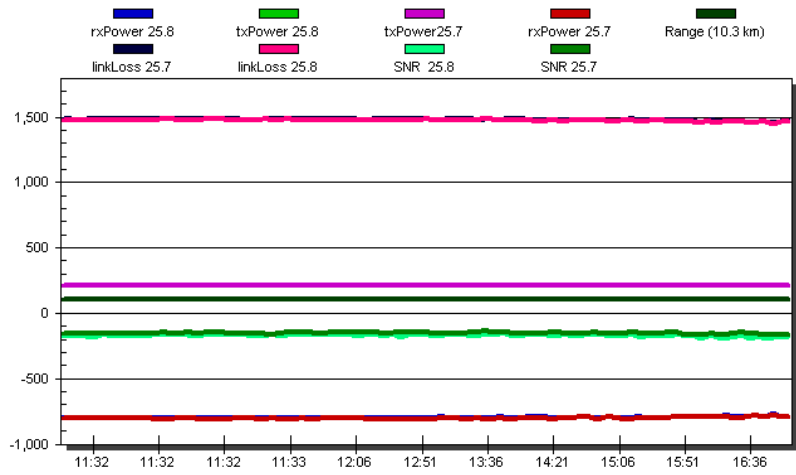


Figure 5. The Solarwinds chart shows available network monitoring parameters.

The conventions of the metrics between the RFMonitor and *Solarwinds* software are different, in term of both received power and the ways that SNR vice SENADR is calculated. A conversion used between Solarwinds and RFMonitor is listed in Appendix C.

2. Meteorological Instruments and Models

a. Mini Rawinsonde System and RS-80 Radiosonde

We took upper air observations using the AN/UMQ-12 Mini Rawinsonde System (MRS) and RS-80L/RS-80G radiosondes. The MRS is a mobile system weighing 66 pounds that includes a computerized receiver/processor, a UHF antenna that receives signals from the RS-80 radiosonde transmitter, and a GPS antenna. Vaisala, a Finland based meteorological instrument company developed the MRS and the RS-80 radiosonde.

During ascent, the radiosondes measure profiles of humidity, temperature, and winds in the upper atmosphere every two seconds. During the

experiment, winds were never recorder due to GPS synchronization problems. The RS-80 radiosonde has a known dry bias and only one humidity sensor (Smout et al. 2005).

Due to an MRS equipment failure, radiosonde data were not available from 21-25 May 2007, until a new unit could be delivered to the test site in Thailand. Table 1 lists radiosonde launches conducted during the experiment along with local times. THA is Thailand Standard Time; THA=UTC+07. Thailand does not observe daylight savings time.

Table 1. Available rawinsonde measurements in THA.

Data Collection Days	Local Time of Rawinsonde Launch
22 Mar 07	0800, 1700 THA
23 Mar 07	0800 THA
26 Mar 07	0800, 1100 THA
27 Mar 07	0700 THA
28 May 07	0900, 1600 THA
29 May 07	0800, 1700 THA
30 May 07	0800, 1300 THA

b. Coupled Ocean/Atmosphere Mesoscale Prediction System (COAMPS)

COAMPS is a mesoscale model developed by the Marine Meteorology Division of the Naval Research Laboratory. COAMPS requires initial fields for calculation of future gridded atmosphere values. These fields are based on combinations of climatology and observations. Observations from satellites, aircraft, surface and upper-air stations, buoys and/or ships are input along with the previous COAMPS 12-hr forecasts. COAMPS uses nested grids in order to achieve high resolution for a given area. It can be run with any number of nested grids (Naval Research Lab 2003).

For this study, we chose spatial resolutions that were high enough to describe most features that are important to overland refraction effects. In our data collection, the four grid resolutions (54, 18, 6 and 2 km) were centered on the Mae Ngat dam area of operations in Thailand. Vertically, COAMPS calculates analysis and forecast variables on terrain-following sigma levels; we used the default of 30 vertical levels for this experiment. The levels are unevenly spaced in order to provide higher resolution in the boundary layer. The COAMPS runs include 10 layers in the bottom 1500m of the atmosphere.

In this set of data, hourly fields of relevant atmospheric parameters are output from 12-hr forecasts initiated at 0000 UTC from 23 March 2007 to 27 March 2007. COAMPS data from the second Thailand experiment included 21-25 May and 28-30 May. Fleet Numerical Meteorology and Oceanography Center (FNMOC) performed two runs at 0000Z and 1200Z for each day of interest. Appendix D lists the requested GRIB fields. GRIB is a packed binary format commonly used in the meteorological community. FNMOC also post-processed the data to produce forecast soundings for locations requested. These files included temperature, dewpoint, wind speed and direction, and refractivity units at 30 pressure levels.

3. Propagation Model Set-Up and Input

The two propagation effects models used to evaluate atmosphere impacts, *Builder* and AREPS, required different information when building the “projects” that the models run. “Projects” within the models depend on system parameters and atmosphere input. Appendix B includes the initial parameters used for the model runs.

Builder allows for either analogue or digital type CommDevices to be added and customized in within the Scenario editor. The analysis section of this report will address the advantages of the modeling a digital device. For the purpose of standardization between AREPS and *Builder*, only the analogue equipment functions were used.

Since this was for an overland application, attention was given to how the models treated the terrain. Barrios (2006) showed the susceptibility of propagation models to different terrain data. To ensure the same terrain data were available in all model runs, Level II Digital Terrain Elevation Data (DTED) was installed for both systems.

B. DATA PROCESSING

At the end of the data collection, four types of measured data were available. These included network data from Solarwinds and RFMonitor, ground measurements from temporarily installed sensors, and radiosonde measurements. The ground weather data was not used, but is available for future analysis. Additionally, COAMPS model data was available and included post-processed vertical profiles.

The primary goal of analyses in this study was to compare propagation model output with measured signal. We designed the study to accomplish this using AREPS and *Builder* with the measured meteorological data, and to then compare the propagation prediction results from each to the corresponding measured signal. Because *Builder* cannot accept radiosonde data, a side-by-side comparison is not feasible.

A secondary goal was to determine how real time propagation conditions could best be accessed and used by forward deployed personnel. Because radiosonde launches are not always feasible, this could involve comparing in-situ radiosonde data with COAMPS predictions. For this comparison, we will run AREPS with the radiosonde data, then with atmospheric profile as predicted by COAMPS at the same hour.

As described, *Builder* requires k-factor as input. So, to have *Builder* in the analysis, k-factors were calculated from the available atmospheric profiles to use as meteorological input. We will run *Builder* with the calculated k-factors and

compare the output to the corresponding measured signal. We will also run both AREPS and *Builder* with the Appendix C variables for a standard atmosphere and compare results.

In data analyses, we also hope to determine whether an average, or “worst case”, value of signal loss due to atmospheric effects can be established. To achieve this we will try to determine if diurnal trends exist in the measured signal data in order to recommend the optimal time for model runs or radiosonde launches in support of operations at 5.8 GHz.

THIS PAGE INTENTIONALLY LEFT BLANK

IV. COASTS 2007 ANALYSIS RESULTS

A. PROPAGATION EFFECTS

1. Propagation Conditions

a. Atmospheric Profiles

Figures 6 and 7 show comparisons of the profiles for each day as measured by the RS-80 radiosonde and as predicted at the same hour by COAMPS. The March COAMPS profiles apply to a grid point (18.78N, 98.98E) that was 20 km away from the balloon launch site, which accounts for the difference in altitude at the lowest data point. Generally, smaller scale features are evident in the radiosonde profiles. These features include non-standard near-surface gradients and elevated trapping layers that are important to propagation.

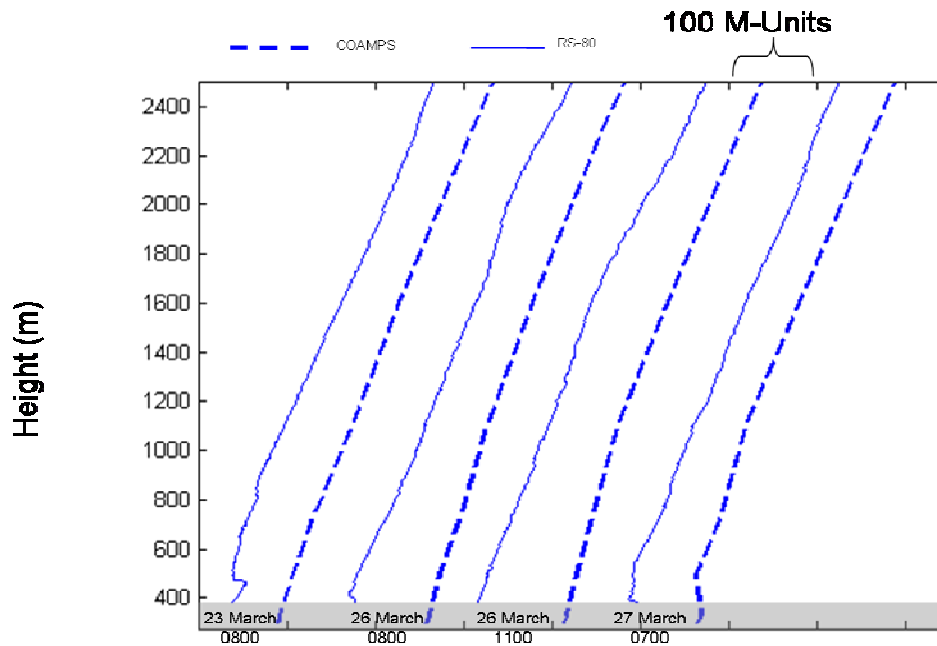


Figure 6. Atmospheric profiles March 23-27 2007, as measured by RS-80 and predicted by COAMPS. The COAMPS in March was set for a position 20 km away from the balloon launch site (18.78N, 98.98E) which is evident in the starting altitude difference.

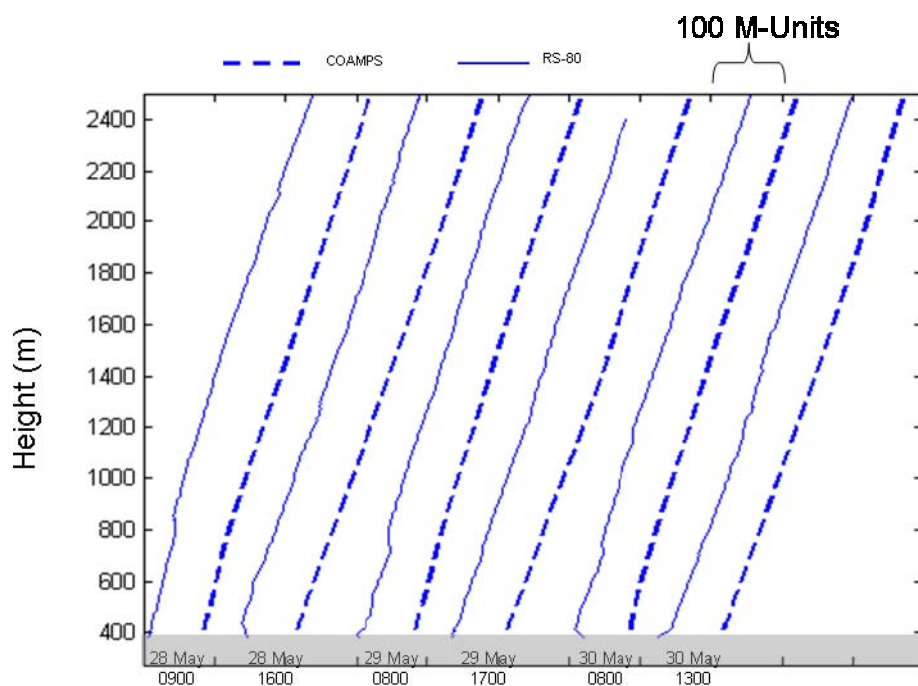


Figure 7. Atmospheric profiles May 28-30 2007, as measured by RS-80 and predicted by COAMPS.

b. K-factor Calculations

As described in a previous section, the Empire portion of *Builder* can use COAMPS GRIB files to perform calculations. Unfortunately, the request to FNMOC for CAAPS did not include all of the required GRIB files. This made this readily performed approach unavailable for the analysis. The meteorological inputs that could be used with *Builder* included a subjective analysis of the ducts in Figures 6 and 7, or calculation of k-factors.

As the profiles showed little ducting, we chose the latter. K-factors were calculated for each radiosonde and COAMPS profile using the values at M_{surface} and those closest to $M_{100\text{m}}$, and $M_{1000\text{m}}$. The k factors from each profile are listed in Table 2. The height, z , is measured from the above ground level (AGL) reference.

Table 2. K-factors calculated for radiosonde profiles and corresponding COAMPS profiles. Points used for the calculation were 100m and 1000m above ground level.

Date	Time	Radiosonde k factor (dz=100m)	Radiosonde k factor (dz=1 km)	COAMPS k factor (dz=100m)	COAMPS k factor (dz=1 km)
23-Mar-07	0800	7.80	1.65	-8.43	1.90
26-Mar-07	0800	-5.67	1.43	3.56	2.00
26-Mar-07	1100	1.43	1.50	1.43	1.81
27-Mar-07	0700	-4.26	1.65	1.53	1.92
28-May-07	0900	1.61	1.71	2.28	1.47
28-May-07	1600	-11.24	1.38	1.17	1.17
29-May-07	0800	0.87	1.40	1.79	1.51
29-May-07	1700	1.18	1.29	1.18	1.17
30-May-07	0800	-3.60	1.65	2.64	1.49
30-May-07	1300	0.60	1.11	1.22	1.21

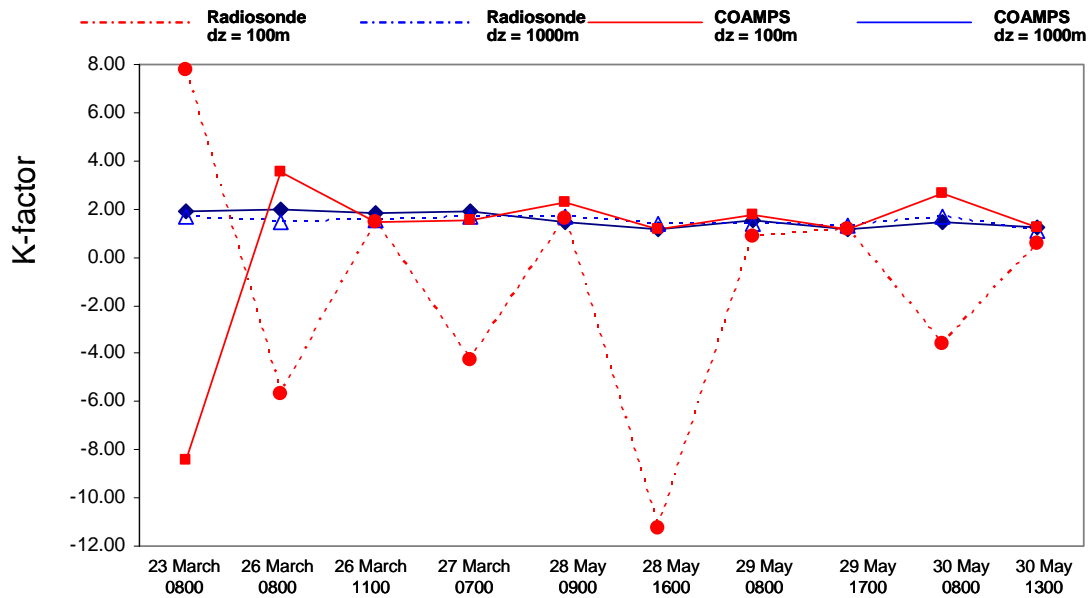


Figure 8. K factors calculated for dz=100m and dz-1000m for each COAMPS and radiosonde profile. Large anomalies are seen at dz=100m.

The variability of the k-factor at 100m is indicative of the presence of ducts or other small-scale processes in the boundary layer. Though these are important for refractivity, the k-factors at this integral scale are unusable, and vary greatly from the frequently used default value of 1.33, which is indicative of a standard atmosphere. The bottom 1000m of the atmosphere was chosen for the calculations. Figure 9 shows the resultant k-factors calculated from the points at z=0m AGL and z=1000m AGL.

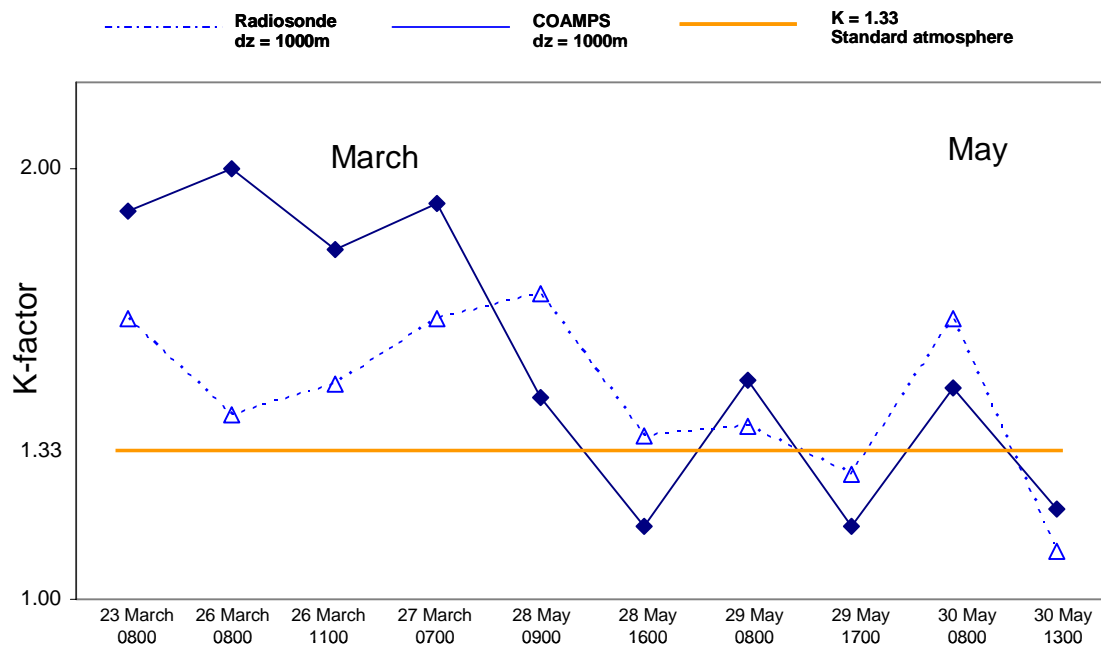


Figure 9. K factors calculated for dz-1000m for each COAMPS and radiosonde profile. Seasonal and diurnal variations are more evident at dz=1000m.

The COAMPS k-factor data show trends between higher values in March and lower values in May. The May results also seem to show a diurnal trend, with k-factors being higher than 1.33 in the mornings, and lower than 1.33 in the afternoons. The lower level radiosonde profiles, from which k-factors were calculated, show this weak diurnal trend.

From results in Table 2, the highest observed k-factor was 2.0, and the lowest k-factor was 1.1. The Mae Ngat network scenario was run in *Builder* with parameters as listed in Appendix B, and the results were compared for the maximum and minimum k-factor with no ducts selected. Calculated values at a range 5.46 nm and at a height of 1400 ft, which correspond to the location of the radio of interest at METG, are shown in Table 3. Originally, the vertical resolution in the visualization tab of *Builder* was set to 30 steps from 0 to 1200 ft AGL, or 40 ft resolution. When the results were not as expected, the vertical resolution was increased to 60 levels, or 20 ft resolution, and finally 385 levels or approximately 3 ft resolution, with 440 range steps, or 41.6 m. The 385 and 440 level values were selected because they are the number of horizontal and vertical steps that AREPS outputs by default. The results in Table 3 show that the vertical resolution impacted the modeled signal loss (dB) more than differing the k-factor at a given resolution. This may imply that a mesoscale model, which has limit on resolution, may not provide accurate impact predictions, if the atmosphere had an impact. The latter has not been established in this thesis.

Table 3. For various k-factors, *Builder* output for signal strength at varying vertical resolutions, or “steps” for the maximum, minimum, and standard k-factor. The vertical resolution affected the signal more than the k-factor used.

k-factor	30 steps	60 steps	385 steps
1.11	-112.75	-112.41	-109.16
1.33	-112.95	-112.11	-109.74
2.00	-114.47	-111.55	-109.66

2. APM Results in a Standard Atmosphere

To establish a baseline comparison between AREPS and *Builder*, standard atmospheres were input to both programs at the Mae Ngat site. AREPS includes a <standard> atmosphere default, defined as 188 M-units/km

(Barrios, personal communication). A standard atmosphere was simulated in *Builder* by deselecting ducts, using a k-factor of 1.33, and keeping ground temperature and humidity defaults.

Figure 10 shows the results of the comparison of AREPS and *Builder* in standard atmosphere refraction conditions. When large differences were apparent at 1400 ft around 5 nm in range, readings were taken at 1600 ft to determine if the anomaly resulted from terrain along the path, as a ridge was present at a distance of 4-6 nm. Figure 12 shows a terrain map with the ridge at the same 10 nm scale. The result of the Received Power plotted with range for AREPS and *Builder* is shown in Figure 10.

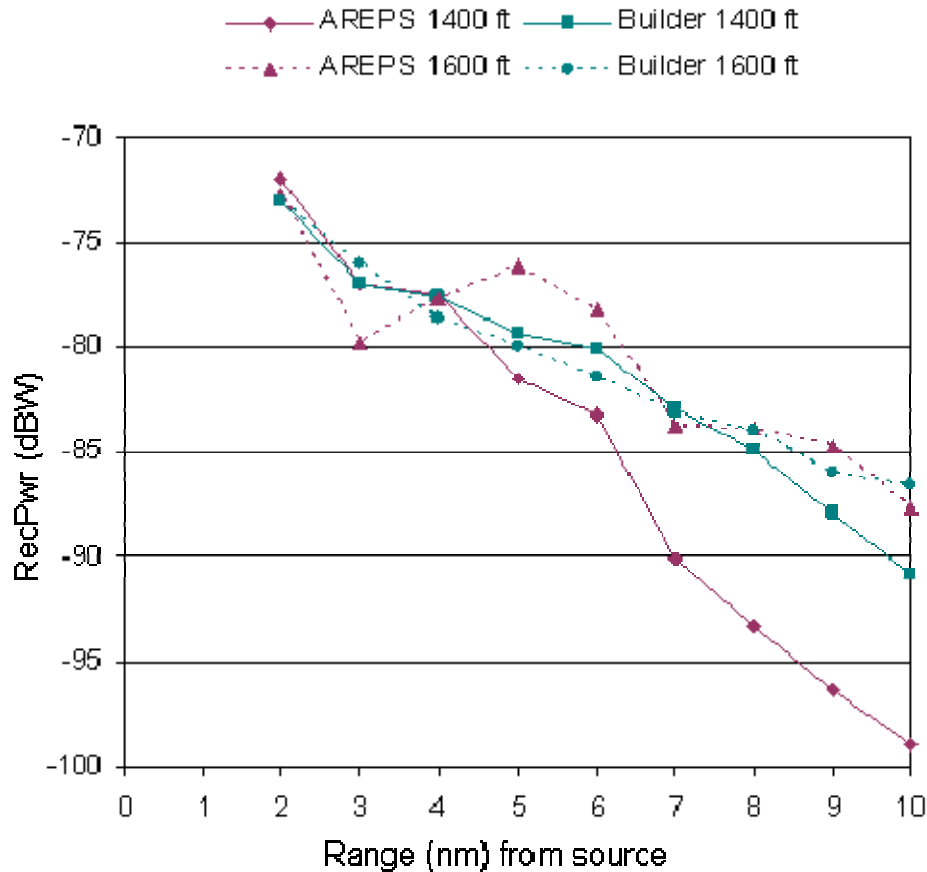


Figure 10. For a standard atmosphere running APM, *Builder* and AREPS dBW at various ranges. The largest difference at 1400 feet may be due to terrain.

The results indicate that though AREPS and *Builder* were both running the APM model, other modeling or visualization capabilities in *Builder* handled the terrain differently. This could be due to the way that *Builder* defines the terrain profile fed into APM, or the older version of APM which EMPIRE uses. *Builder* showed similar trends in received power at the 1400 and 1600 ft altitudes, while AREPS received power at the different altitudes varied by as much as 11.3 dBW at 10 nm.

A second comparison of received power and range at 1400 ft altitude was completed using profiles from a single day. Only AREPS was used to determine the predicted difference between a COAMPS and radiosonde profile for 30 May at 0800. Again, readings were taken at 5.46 nm, at 1400 ft. Figure 11 shows a difference of over 3 dBW at a range of 5 nm (in the vicinity of the terrain feature) between the model output from a COAMPS prediction and Radiosonde launch.

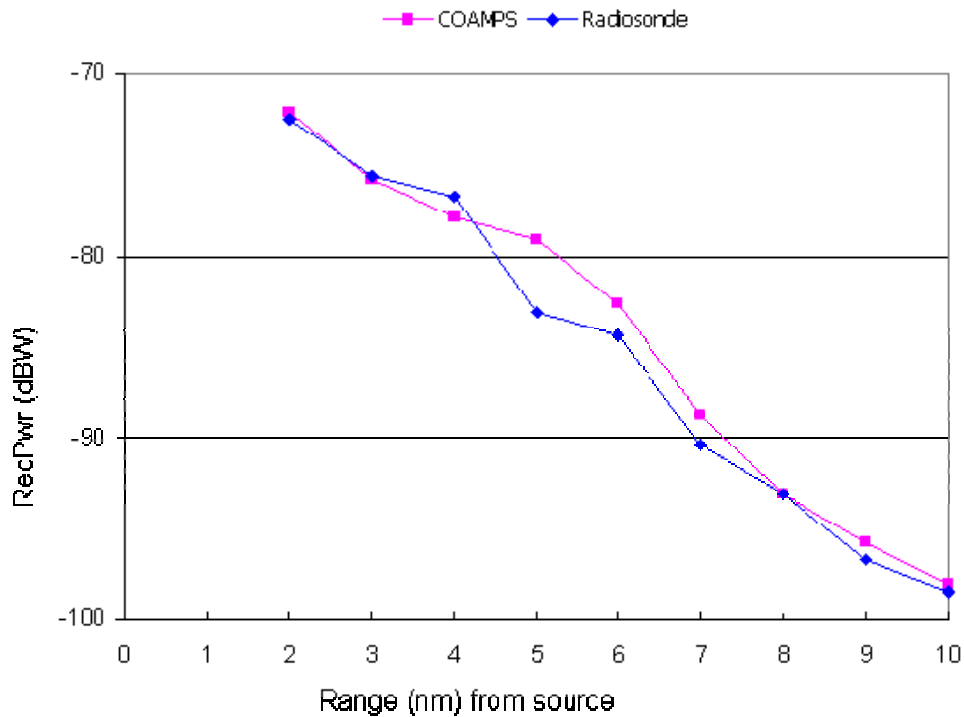


Figure 11. AREPS outputs for 30 May 0800 at ranges of 2-10nm from the radio source at Mae Ngat. Environments used were COAMPS analysis for 30 May 0800 and in-situ Radiosonde launch at 30 May 0800. The largest loss difference is 3 dBW at a distance of around 4-6nm.

Figure 12 shows the terrain feature in vicinity of the deviations at 4-6 nm from the radio source.

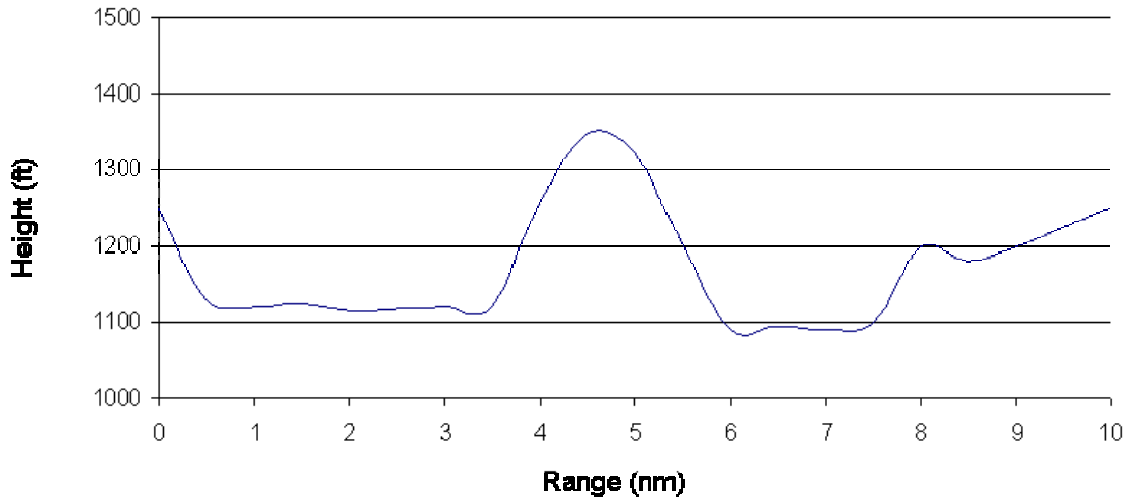


Figure 12. Terrain heights from Mae Ngat radio site, showing ridge from 4-6 nm.

3. TDA Results vs Observed Propagation Loss Results

In this section, comparisons between predicted atmosphere impact and network received power are examined. This examination requires several steps, including a description of measured received power. Then the values and trends of predicted loss from propagation model are applied to different type data, and received power is compared with that measured.

a. Trends in RF Data

Figure 13 shows Redline and Solarwinds data for one day. The goal was to establish trends to determine if a diurnal variation could be established as was recognized in the k-factor calculations. Because the measurements were in different units, the Solarwinds data were modified by a factor of $x/10 + \text{antenna gain}$ in order to show trends with RSSI.

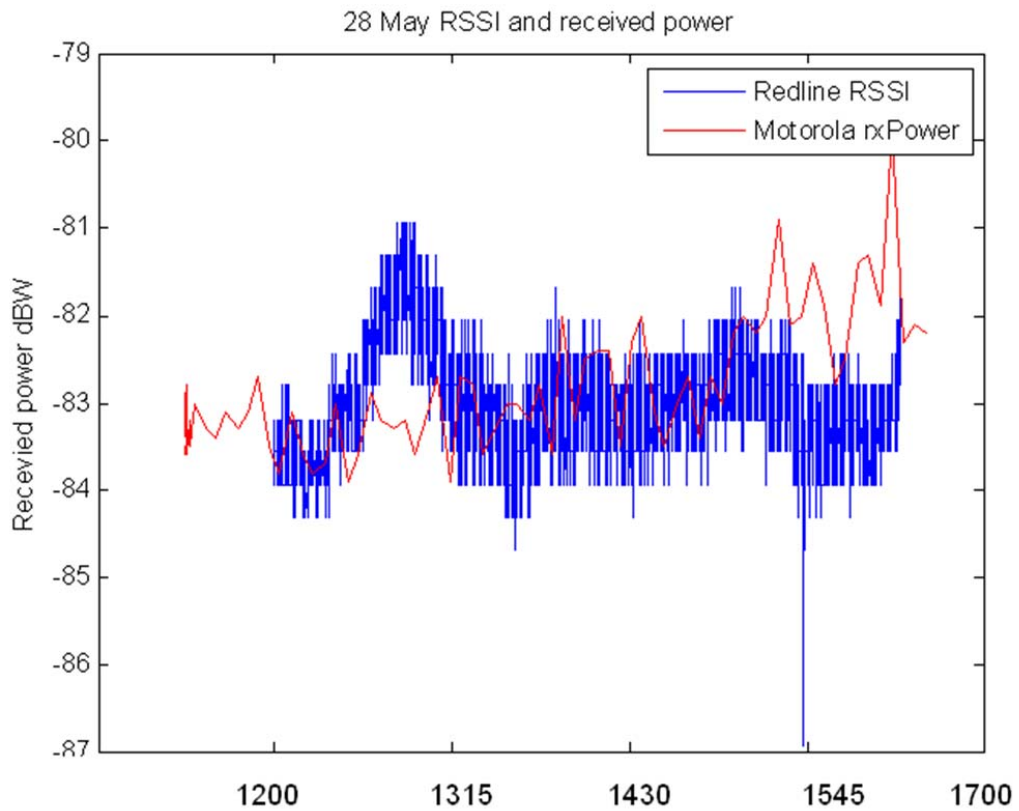


Figure 13. Received power signals recorded from Solarwinds (Mae Ngat) and RFMonitor (METG) radios on 28 May 2007.

In order to eliminate noise, mean signal strengths were calculated hourly for each station. To analyze the received signal strength in context of the k-factor, hourly averages were computed for each day. These are shown in Figure 14.

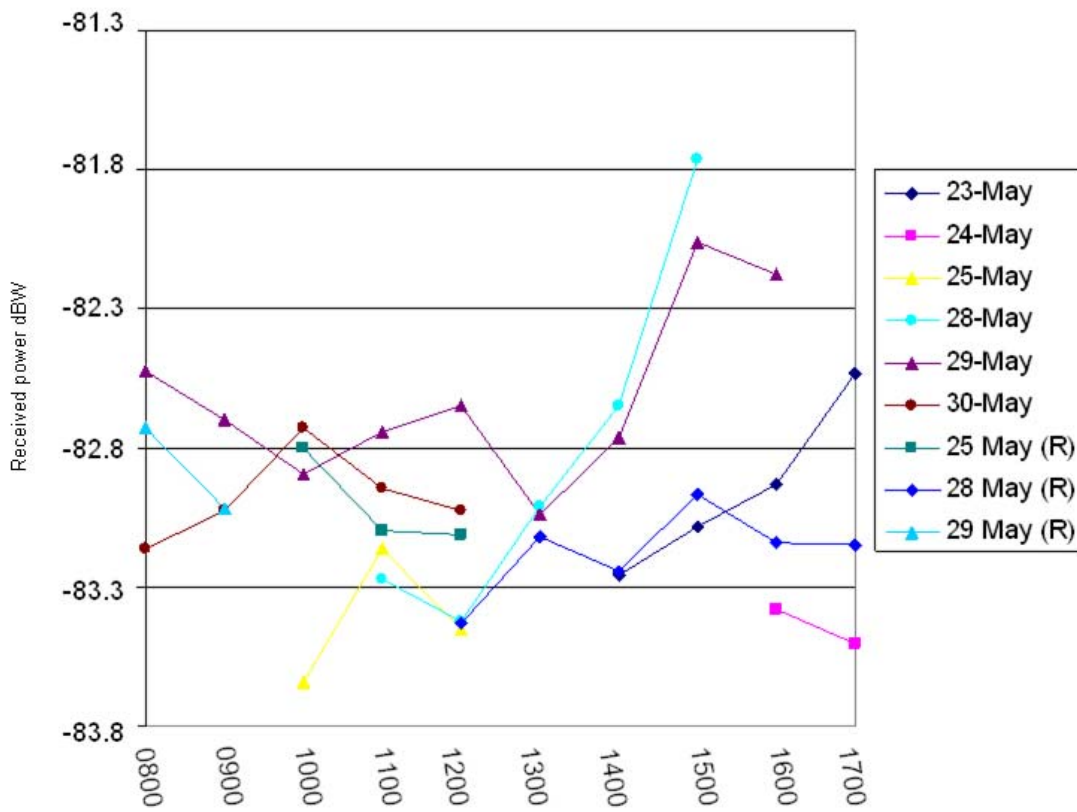


Figure 14. Hourly means plotted for each day of Received signal measurements. The (R) indicates Redline RSSI, with a correction factor added to bring to the same scale as Motorola rx power. The highest signals were often seen in the mid-afternoon.

The next step was to take the hour-by-hour average of each day's signal and compare it to the mean of all of the hourly averages. The lowest received signal levels occurred around 1200, while the highest received signal levels occurred around 1500.

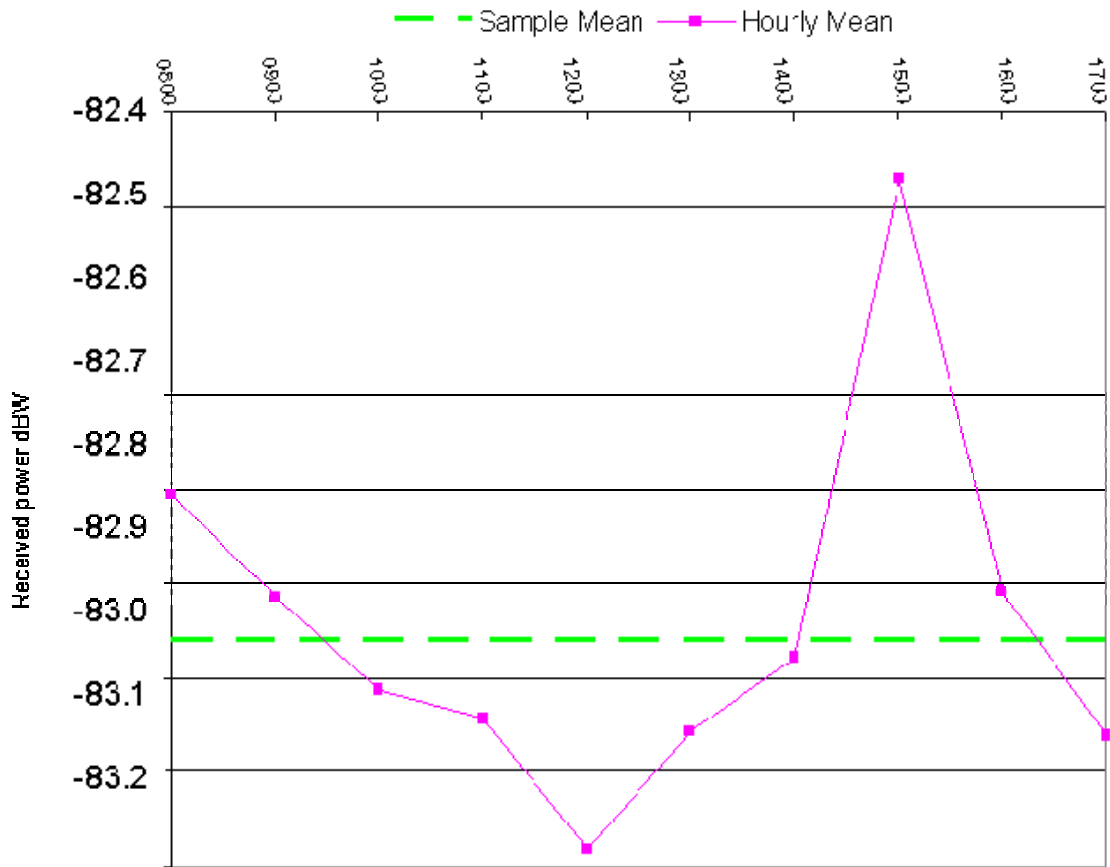


Figure 15. Hourly means plotted, averaged over every day of received signal measurements. The period of 1000-1300 showed below average signal strength.

b. Hourly Received RF vs APM Predicted Power

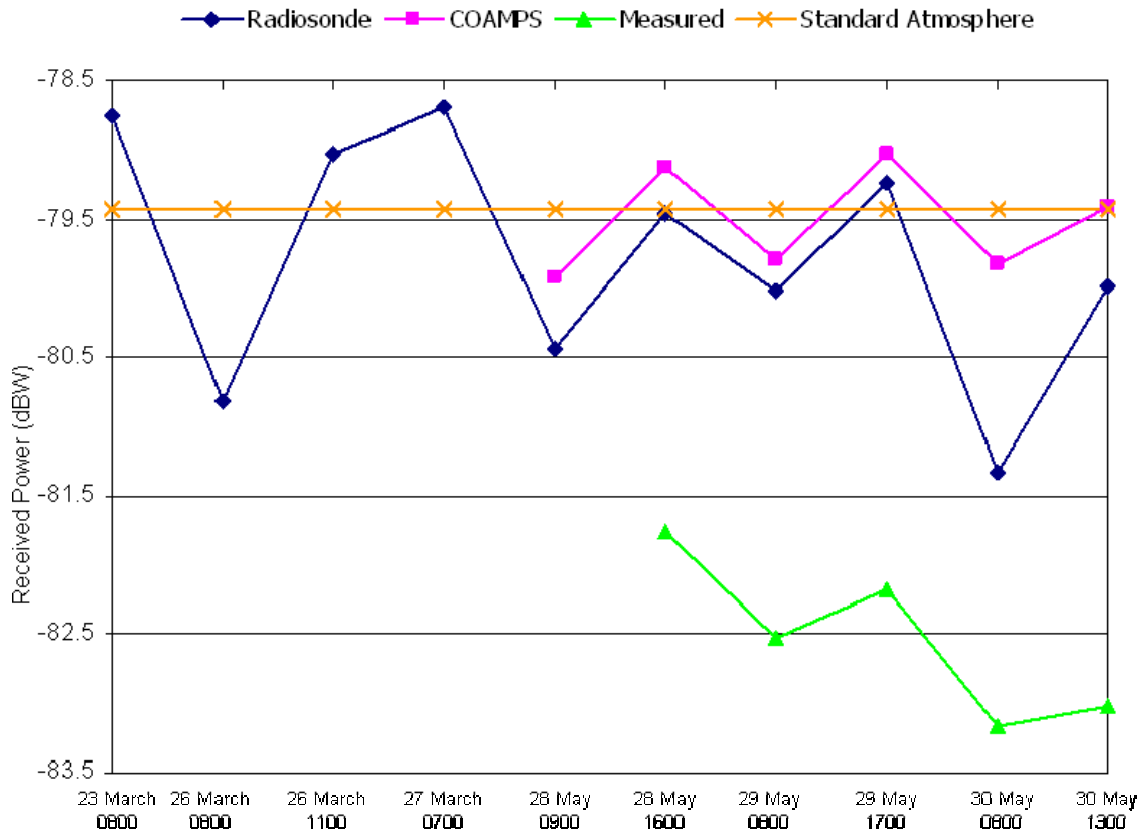


Figure 16. Plot of AREPS predicted receive power based on COAMPS and radiosonde profiles, and measured signal from the Motorola 600 with Solarwinds.

Hourly mean observed signal from Solarwinds for the time closest to the radiosonde launch along with the AREPS predictions for the predicted signal strength were plotted together. Comparison of curves in Figure 16 reveals that the signal strength trend generally follows the diurnally forces shape of the AREPS predictions, for both Radiosonde and COAMPS data input. The mean AREPS-radiosonde calculated signal for the 1600 28 May – 1300 30 May points is -80.01 with a standard deviation of .81. The mean AREPS-COAMPS calculated signal for the 1600 28 May – 1300 30 May points is -79.5167 with a standard deviation of .39. The mean measured signal was -82.53 dBW with a standard deviation of .59. The explanation for the lower mean of the measured

signal is that I used 0dB for the “assumed system loss” in AREPS and *Builder* in order to standardize the input and to use the fewest assumptions. As discussed in Chapter II, system losses are inherent in a communications system due to physical factors such as cabling or connectors. This could explain the bias that is evident in the comparison.

The radiosonde-derived results show a lower minimum on 30 May than on 29 May, which agrees with received power variations. The lower amplitude variation in the measured data as compared to the AREPS-radiosonde predicted signal could be due to the digital signal modulation. The transmitted signal was actually digital OFDM, which has an increased capability for multi-path; however, AREPS only models analogue signals.

Variation in the atmospheric impact was not expected to be a factor in the network performance given the relatively short distances between radios, four of five of which were line of sight. However, Figure 16 displays propagation model losses which were realized in the actual received signal data. This could be due to the terrain influence in the Mae Ngat – METG link. Varying atmospheric gradients cause wavefront tilts and therefore affect the angle at which the wavefront is reflected by the terrain. The propagation model is therefore useful in determining whether a signal could clear the Fresnel zone given varying atmospheric conditions at a given antenna height.

B. ATMOSPHERIC AND EFFECTS BASED MODELS IN ISR PLANNING

1. AREPS and *Builder* Comparisons

An operational-use based appraisal shows that AREPS and *Builder* are useful effects based models for predicting EM propagation. The visualization tools that each system provides, allow for a comprehensive understanding of the RF coverage of a given area with respect to terrain features. The documentation for both AREPS and *Builder* provide adequate background, instructions, and illustrations for a first time user to become proficient with the software. The differences that exist in usability and visualization are outlined below.

A main advantage of *Builder* is its present ability to model digital signals. This capability was not thoroughly analyzed in this study, as it could not be compared to AREPS in this configuration. When a function is added for a digital CommDevice, available inputs include Modulation Type, Bit rate, Ideal and Max Bit Error Rate (BER), Minimum and Ideal E_b/N_0 , a ratio of energy per bit to spectral noise density, and Detection type. The digital option allows for varying modulation types, such as Quadrature Phase Shift keying, though OFDM is not yet an option. This is a useful tool for communications engineers. There could be some discrepancies with this feature in the vicinity of terrain. For example, the BER plots did not show any appreciable loss behind topography where the corresponding SNR plots showed a significant loss of signal.

AREPS unit conversions are easy to use. In *Builder*, though the user can change the range of a plot to a given number in km, for instance, the plot itself still carries all units in nm. Similarly, *Builder* only allows surface humidity inputs in g/m^3 , while AREPS includes a unit conversion tool for relative humidity, absolute humidity, dewpoint, and other moisture variables. Other advantages of AREPS include easy manipulation of color scales, and its straightforward ASCII text files for data analysis.

Software versions of both effects based models are available to registered users and easily downloadable. The AREPS support page lists the current release and changes, while the *Builder* site states the current release, but ambiguity exists as to the date of the most recent patch or what changes were made.

Builder allows various display options especially for 3-dimensional visualization, and includes installed map packs for easy geographical reference. Figure 17 is an example of *Builder's* display capabilities. AREPS' inclusion of Falcon View software also allows for three-dimensional viewing and is useful in the DoD, as Falcon View is widely used in Joint flight mission planning.

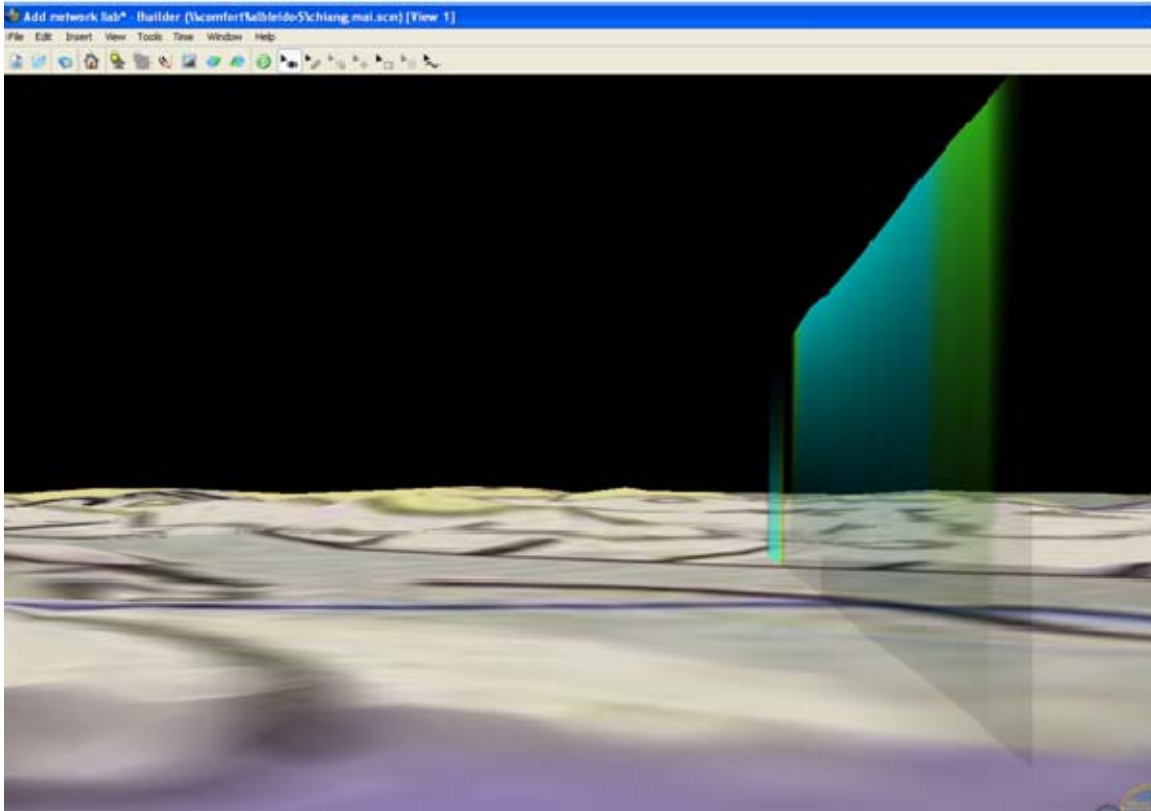


Figure 17. *Builder* diagram showing terrain. View is from METG tower looking back.

Discrepancies exist in both programs, which are notable from a troubleshooting aspect. First, while AREPS shows the capability to display an SNR diagram; it only will perform calculations with a bandwidth of 10 Hz, which is unrealistic for any wireless networking scenario. The SNRs on the graph will read too high. The SNR must be calculated by hand using the actual bandwidth.

In *Builder*, the result of any manual wind input over 20 knots results in a complete loss of signal. From 0 to 19.9 knots there is a reasonable .5 dBW drop. Also in *Builder*, changing the Noise temperature from the default of 77 degrees down to 0 F and up to 200 F does not appear to affect noise level at any range given the inputs in Appendix C.

While these factors are minor, the main concern with a model comparison lies in accuracy. The ability to choose low resolutions in *Builder* can greatly

affect model output, as shown in Table 3. Where terrain is involved, it is important to run *Builder* with the highest possible resolutions based on the available processing, and the user should be alerted to concerns with choosing fewer “steps”. Running *Builder* with actual calculated k-factors was not a realistic measure of expected loss. This method is not recommended in the future as a meteorological input over short ranges near appreciable terrain. It is highly unlikely that even with a radiosonde profile that the duct height and strength could be chosen appropriately. Subrefraction is not an option as a condition, except by selection of a correlating k-factor. Therefore, when using *Builder*, it is obviously important to have all of the required COAMPS GRIB files to properly evaluate the RF conditions caused by the atmosphere. It is unfortunate that the current *Builder* system does not have the capability to process radiosonde profiles for inclusion into the APM model in EMPIRE.

V. SUMMARY

A. DISCUSSION

Wireless communications infrastructures can greatly enhance situational awareness during military operations. The 802.16 protocol provides a capable backhaul for information sharing. To this end, we wanted to determine how of if atmospheric conditions can negatively influence this situational awareness due to any loss of the 802.16 signal. We compared received signal strength measurements taken from an 802.16 network at the Mae Ngat dam during COASTS 2007 with atmosphere propagation effects based model predictions. Received signal strength and meteorological data spanned several days and various refractive conditions. The received signal data show a correlation with AREPS predicted signals for both in-situ and COAMPS profiles.

The study was based on initially posed research questions. The first question was whether Electro Magnetic propagation models could be used to predict the performance of wireless networks. An original hypotheses was that due to the wavelength and short range of our network, atmospheric variables would play little role in the received signal strength. However, in the vicinity of terrain, even at a distance of 5.46 nm between radios, refractive effects seemed cause the signal to vary in the vicinity of a blocking ridge at the edge of the Fresnel zone. In the presence of significant terrain we found that AREPS and APM are useful tools for RF prediction, even at short distances. Further, it is recommended that *Builder* add the capability to use in-situ data from radiosondes and include better tools for data analysis and research in order to determine its accuracy in this area.

Another desired outcome of the study was to determine an average value of signal loss due to atmospheric variables that network planners could use in the absence of real-time meteorological data. A maximum of 3 dB variation in AREPS output at 5.4 nm, given six days of radiosonde data; was observed.

However, the variance is greater around terrain, and may change in various monsoon phases. AREPS climatology already includes the ITU recommendations for world-wide refractivity by season, which is of a much larger scope than this study.

Two other considerations can be added here. One is that from the network engineer's perspective, signal loss is not always the deciding factor in network installation and topology planning. In the case of COASTS '07, the original question was how high of a tower needed to be built at Mae Ngat to maintain radio communications with the next link at METG. In this case, during the planning phases the models could have been run for a lowest acceptable antenna height instead of trying to determine the maximum signal loss that the atmosphere could cause. The second consideration is that at times planners need to consider the most favorable propagation conditions in order to prevent enemy intercept or friendly interference. Ducts and best case conditions need to be considered in these instances. In summary, the original question oversimplified the requirements for meteorological input.

A third research goal in this study was to determine how real-time propagation conditions can be best accessed and used by forward deployed personnel. Unfortunately, though called the Mini-rawinsonde system, the AN/UMQ-12 is a cumbersome unit requiring trained personnel and sometimes hard to acquire peripherals such as helium for the balloon launches. Though smaller variants of radiosondes and receiver units are available, easier to deploy sensors for upper air observations should remain a priority. It is for these reasons that COAMPS predictions for atmosphere conditions were part of this study. It was shown that, in the absence of real-time data, COAMPS refractivity profiles were more accurate than assuming a standard atmosphere. Though COAMPS "missed" small gradients in the M profiles detected by the RS-80, its overall performance showed that it reasonably matched the measured received signal. In this application, COAMPS data was sufficient for determining loss; however, in other scenarios involving longer ranges, different terrain, or support

to other military missions, the in-situ measurements provided by radiosondes could be a determining factor in determining network topology and requirements.

Lastly, a question is “how can the military’s meteorology and oceanography communities best support a network system that is needed for Intelligence, Surveillance, and Reconnaissance (ISR) missions.” Specifically in the realm of supporting networks, it is important for those assigned to support missions dealing with RF propagation to be familiar with tools and terminology as new technology emerges. Additionally, support personnel should consider the use of these planning tools in all warfare areas and become involved at the planning phases. For example, during Exercise Talisman Saber 2007, an 802.16 wireless network was established between Expeditionary Strike Group ships and a ground station in support of Marine landing operations (Wren 2007). Understanding what tools are available for RF propagation and sharing the products will become increasingly applicable as even more military operations take advantage of the capabilities of wireless networks. It is also important to understand and brief the limitations of the effects based models. For example, neither AREPS nor *Builder* includes information on vegetation or urban structures that can greatly affect propagation. Another possibility in supporting operations is to consider the use of a stochastic vice deterministic propagation forecast. For instance, instead of presenting only the forecasted RF propagation loss in dB, planners could be given the probability that the worst case propagation loss may occur. Ultimately, understanding the value that RF propagation models can add, and understanding the specific network topology challenges for a given time and place, will result in the best support to network planning for ISR.

B. FUTURE RESEARCH

The primary effects based model that requires additional research is the use of EMPIRE/*Builder* with COAMPS data. This study could include more types of digital and analogue communications links in varying terrains and seasons.

Additional research could also include specific 802.16 signal measurements over water, and determining the effects of ducts on the signal propagation. Waterborne or mobile testing could be possible with the use of a computer code written to take measurements from the mobile target stamped with time, GPS location, and signal strength.

A more detailed comparison of modulation types and additional time series of signal-strength data will greatly aid in understanding the extent of the atmospheric effects on the wireless networks and digital signals of the future. A truly multi-disciplinary study in this area is recommended, including experts in electrical engineering and antenna performance as well as personnel proficient in network design and Simple Network Mapping Protocols.

The COASTS 07 meteorology team collected ground based data. Analyses can be conducted on variations in irradiance, winds, temperature, or humidity at smaller time scales and their resultant effect the 802.16 network performance. A more robust analysis of the available COAMPS fields as listed in Appendix D could also determine whether COAMPS is an adequate substitute for in-situ upper air soundings.

Future field testing should consider additional radiosonde launches around the time of the highest signal strength variability; in the case of COASTS '07 this was around 1200. Also, the use of equipment such as a spectrum analyzer would be ideal for determining exact propagation losses, vice using the software to record transmitted and received power, and determining factors to compare measurements of different units.

LIST OF REFERENCES

- Alexander, Bruce, 2005: *802.11 Wireless Network Site Surveying and Installation*. CISCO Press, 432 pp.
- Atmospheric Propagation Branch, SPAWAR SSD, 2006: User's Manual for Advanced Refractive Effects Prediction System, 294pp.
- Barrios, A. E., 2003: Considerations in the Development of the Advanced Propagation Model (APM) for U.S. Navy Applications. *Proc. IEEE Conf. on Radar*, 6 pp.
- Barrios, A.E., K. A. Anderson, and G.E. Lindem, 2006: Low Altitude Propagation Effects - A Validation Study of the Advanced Propagation Model (APM) for Mobile Radio Applications. *IEEE Ant. & Prop.*, **54**, pp. 2869-2877.
- Battan, L.J., 1973: *Radar Observation of the Atmosphere*. University of Chicago Press, 324 pp.
- Bean, B.R, and E.J. Dutton, 1966: *Radio Meteorology*. United States Department of Commerce, Washington, D.C. 431 pp.
- COASTS Program, Naval Postgraduate School, April 24, 2007: COASTS Concept of Operations 2007, Monterey, CA, 98 pp.
- Cooklov, T., 2004: *A study of IEEE 802.11, 802.15, and 802.16*. Wireless Communications Standards Series, IEEE Press, 360 pp.
- Davidson, K. L., 2003: *Assessment of Atmospheric Factors in EM/EO Propagation*, Course Notes, Department of Meteorology, Naval Postgraduate School, Monterey, California.
- Dodgett, M, 1997: An Atmospheric Sensitivity and Validation Study of the Variable Terrain Radio Parabolic Equation Model. M.S. Thesis, Air Force Institute of Technology 94 pp.
- Harvey, R., 1987: Subrefractive fading model for microwave paths using surface synoptic meteorological data," *IEEE Transactions on Antennas and Propagation*, **35**, 832-844.
- Higdon, Melody, 2004: Thailand, a Full-year study. Air Force Combat Climatology Center, Ashville, NC, 54 pp.

- Hitney, Herbert V, J.H. Richter, R.A. Pappert, K.D. Anderson, G.B. Baumgartner Jr, 1985. Tropospheric radio propagation assessment. *Proceedings of the IEEE*. **73**, 265-283.
- Institute of Electrical and Electronics Engineers, Inc: 2004. Air Interface for Fixed Broadband Wireless Access System, IEEE Std 802.16-2004. 857pp.
- Levy. M.F. and K.H. Craig. Case studies of transhorizon propagation: Reliability of Predictions using Radiosonde Data. *Sixth International Conference on Antennas and Propagation*. **2**, 456-460.
- Miller, C., 2006: Statistical Analysis of Wireless Networks: Predicting Performance in Multiple Environments. M.S. thesis, Dept. of Operations Research, Naval Postgraduate School, 56 pp.
- Myers, W: 1999. IEEE P802.16 Broadband Wireless Access Working Group Comparison of Propagation Models. Available at: [http://www.ieee802.org/16/tg2_orig/] last date accessed, March 2008.
- Naval Research Laboratory, May 2003: COAMPS Version 3 Model Description. NRL/PU/7500—04-448, Monterey, CA, 143 pp.
- NAVEDTRA 14270 *Aerographer's Mate Module 2-Miscellaneous Observations and Codes*. NETPDTTC 1550/41 (Rev 4-00), April 1999.
- Oraizi, H.; Hosseinzadeh, S., 2003: "The effect of atmospheric duct on modern OFDM-based digital broadcasting systems," *33rd European Microwave Conference*, **2**, 747-750.
- Paulus, R. A.: 1995. An Overview of an Intensive Observation Period on Variability of Coastal Atmospheric Refractivity, AGARD Conference Proceedings, **567**, 386-388.
- Rao, D.; Murthy, M.; Sarkar, S.; Pasricha, P.; Dutta, H.; Reddy, B., 1987: Hilly terrain LOS fadeouts and Fresnel zone considerations from ray tracing techniques. *IEEE Transactions on Antennas and Propagation*, **35**, 1330-1333.
- Remcom, Inc., July 2003: A Basic Guide for Electromagnetic Wave Propagation Models. [Available at <https://builder.nrl.navy.mil/>] last date accessed, March 2008.
- Rinehart, R. E., 1991: *RADAR for Meteorologists*. University of North Dakota, ND, 334 pp.

Schelleng, J.C., C.R. Burrows, E.B. Ferrell, 1933, Ultra-Short-Wave Propagation, *Proceedings of the IRE* , **21**, 427-463.

Smout, R., J. Nash, T. Hewison, M. Smees, 2005, Results of the RS92 Acceptance Test performed by the Met Office (UK). *World Meteorological Organization Technical Conference on Meteorological and Environmental Instruments and Methods of Observation – TECO 2005*. [Available at http://www.wmo.ch/pages/prog/www/IMOP/publications/IOM-82-TECO_2005/Programme_index.html] Last accessed September 2007.

Wilks, D. L., 2006. *Statistical Methods in the Atmospheric Sciences*. Elsevire. San Diego, 627 pp.

THIS PAGE INTENTIONALLY LEFT BLANK

APPENDIX A - INPUTS TO PROPAGATION MODELS

Table 4. *Builder* Communications project, antenna and emissions initial inputs

Antenna - MaeNgat

Antenna pattern:	Sinx/x
Height	15m
Polarization:	Vertical
Max Gain:	28 dBm
Sidelobe Gain Offset	-25 dBm
Beamwidth (Azimuth)	6 deg
Beamwidth (Elevation)	6 deg
Position Azimuth	241 deg
Position Elevation	15m AGL
X/Y offset:	0 m
Z Offset:	50.0 ft/15m

Emissions – MaeNgat

Tx Frequency:	5.8 GHz
Tx Bandwidth:	200 MHz
Peak Power:	21 dBm
Rx Frequency	5.8 GHz
Rx Bandwidth:	200 MHz
RX Noise figure:	1 dB
Min. Discernible SNR	8.0 dB
Ideal SNR	10 dB
Minimum J/S	3 dB
Noise temp:	77 F
System Loss:	0 dB
Propagation type:	BER
Propagation Model:	APM
MetOc Effects:	various
Noise type:	No Noise

Plot

Height	0-1200ft AGI
Height divisions	120 *
Range sampling rate	.25641 nm
Azimuth	240-242

Table 5. AREPS Communications project, frequency and display initial inputs

TOC

Vertical beam Width	6 deg
Antenna Elevation angle	0 deg
Antenna height (AGL)	15 m
Polarization:	Vertical
Antenna type:	SinX/X
Frequency	5.8 GHz
Bandwidth	200 MHz*
Assumed system loss	0 dBm
Transmitter power	21dBm
Receiver sensitivity	dBm
Max xmit antenna gain	28 dBm

APPENDIX B – SNR/POWER CONVERSIONS

Equations:

$$P_n = -203.97\text{dBW} + 10 \cdot \log_{10}(\Delta f) + N_f$$

$$P_r = P_t + G_t + G_r - L_{\text{apm}} - L_{\text{sys}} - L_{\text{cp}}$$

$$\text{SNR (dB)} = P_r(\text{dB}) - P_n(\text{dB})$$

$$\text{dBW} = \text{dBm} - 30 \text{ dB}$$

Definitions:

P_n = Noise power in dBW

P_r = Receiver power in dBW

P_t = Transmitter power in dBW

G_t = gain of transmitting antenna in dBi

G_r = gain of receive antenna in dBi

L_{apm} = propagation loss from APM in dBW

L_{sys} = assumed or miscellaneous system losses in dBW

L_{cp} = cross polarization loss (0 for antennas of same polarization)

N_f = noise figure in dBW

$P_{\text{resistor-noise}}$ = defined as -203.97 dB in AREPS

Δf = bandwidth in Hz

AREPS xmit power = Signal strength(*Builder*) + antenna gain – 3dB

RcvPwr = Redline RSSI = (Solarwinds Received Power – antenna gain) / 100

THIS PAGE INTENTIONALLY LEFT BLANK

APPENDIX C – CAAPS SUPPORT REQUEST

Date: 09 May 2007

1. Requestor:

Prof. Kenneth L. Davidson
Naval Postgraduate School
831-656-2309
kldavids@nps.edu

Mary S. Jordan
Naval Postgraduate School
831-656-7571
jordan@nps.edu

2. Purpose of request (mark all that apply):

- Operation - Name: **Cooperative Operational Applied Science and Technologies Studies (COASTS)**
- Exercise - Name: **COASTS-07**
- R&D - Explain below:
 - Investigate net-centric information management and Effects Based Operations (EBO) in a multi-national environment across tactical, operational, and strategic domains
 - Make ISR data and information visible, available and usable when and where needed (iCOP)
 - Create synergy with the Theater Security Cooperation Plan and supporting theater objectives (long-term influence)
 - Expand the scope of maritime research into improved command and control (C2) technologies for Maritime Interdiction Operations (MIO)
 - Investigate deployment issues surrounding hastily formed networks in rugged and varied terrain under adverse climatic conditions
 - Increase situational awareness for the disadvantaged (tactically-engaged) user, and improve the bi-directional flow of information between forward employed personnel and their tactical, operational, and strategic operations centers and headquarters
 - Investigate the dissemination, parsing, protection, security, and sharing of information between various U.S., international, and commercial partners
 - Partner with U.S. Pacific Command (USPACOM), Commander, Pacific Fleet (COMPACFLT) and COMSEVENTHFLT to integrate selected COASTS technologies into exercise TALISMAN SABER-07
- Other - Explain below
 - This test will be used, specifically, to validate the AREPS Electromagnetic propagation model using both COAMPS and in situ data.
 - Show a statistically significant correlation between AREPS predicted signal loss at 2.4/5.8 GHz and observed signal loss over a given range.

3. Classification of this request (if Classified provide Derivative and declass info):
UNCLASSIFIED

4. Data to be made be avail on SIPRNET, NIPRNET, JWICS (circle one). **NIPRNET**

5. Required Start/End date for this support: **12Z 21MAY 07 - 12Z 31MAY 07**

6. Location (Provide NW/SE corner of each of the meshes you will use for applications/forecasting):

Same model setup as for NPS_Thailand CAAPS project in April 2007

7. Resolution desired: **4 nests: 54/18/6/2km (same as previous setup)**

8. Forecast time: **24 hours for each mesh**

9. Availability time (Z) Note: Project requires running after +2 hours in order for observations to be include in analysis.

No requirement. NPS is using the dataset for post analyses, rather than in real time.

10. What applications do you intend this data to be used for (i.e. AREPS, HPAC, forecasting)?

Run AREPS or *Builder* and compare results with in situ measurements. Data set will be used for NPS M.S. Theses. Our plan is to use the skew-T ascii profiles provided for the location points listed in #13.

11. List any specific model fields required (cloud cover, precip, EM ducting, etc...)

A. Selected GRIB fields for Pressure Surfaces, 1013-850 mb, listed in the following table. Save Mesh 1 at 6-hr intervals, Mesh 2 at 6-hr intervals, Mesh 3 at 3-hr intervals, and Mesh 4 at 1-hr intervals.

Air Temperature (kelvin)	airtmp
Dew Point Depression (k)	dwptdp
Geopotential Height	geopht
Relative Humidity	relhum
True U-Velocity Component	uuttrue
True V-Velocity Component	vvtrue
Water Vapor Pressure	vpress

B. Selected GRIB fields for Height Levels, 2-2,000 m, listed in the following table. Save Mesh 1 at 6-hr intervals, Mesh 2 at 6-hr intervals, Mesh 3 at 3-hr intervals, and Mesh 4 at 1-hr intervals.

Air Temperature (kelvin)	airtmp
Dew Point Depression (k)	dwptdp
Em Duct Strength	emdcst
Em Duct Thickness	emdcth
Em Duct Top	emdctp
Relative Humidity	relhum
True U-Velocity Component	uuttrue
True V-Velocity Component	vvtrue
Water Vapor Pressure	vpress

C. Selected GRIB fields for the Surface listed in the following table. Save Mesh 1 at 6-hr intervals, Mesh 2 at 6-hr intervals, Mesh 3 at 3-hr intervals, and Mesh 4 at 1-hr intervals.

Bucket Total Precipitation	ttmlpcp
Ground / Sea Surface Temperature	grdtmp

Ground Wetness	grdwet
Latent Heat Flux	lahflx
Planetary Boundary Layer Height	pblzht
Scale Mixing Ratio For Surface	qqstar
Sea Level Pressure	slpres
Sea Surface Temperature	seatmp
Sensible Heat Flux	sehflx
Surface Roughness	roughl
Terrain Height	terrht

- D. Standard forecast graphics charts.**
- E. CODA graphics charts.**
- F. Observations (OBS) graphics charts.**

12. Do you plan to request NAVO support based on CAAPS/COAMPS output? (Y/N) **No.**

13. Do you require meteogram and/or forecast skew-t graphic products (give locations)? **Yes.**

The names listed are acronyms for antenna towers used in the COAST Experiment. These points replace points used in the April 2007 model setup.

Name	Latitude Decimal Degree	Longitude Decimal Degree	Meteogram	Skew-T and ASCII listing
MNDAM	19.16253 N	99.03917 E	Yes	Yes
METG	19.11830 N	98.95470 E	Yes	Yes
CHCM	18.86629 N	98.96786 E	Yes	Yes
IIFC	18.84670 N	98.96740 E	No	Yes
WING41	18.77417 N	98.97083 E	No	Yes

14. Do you require any custom graphic visualizations of the COAMPS output? (i.e. 1,000 ft winds with RH, cloud base height, etc...) **No.**

15. Do you need data available for METCAST download? What Fields? **No.**

16. Notes/explanation:

Method to get the files from the CAAPS system to NPS. For the April 2007 AUTECH CAAPS-2 run, Tom Neu and Dennis Dismachek created scripts to tar and zip each model run and add the tarred/zipped files to a directory accessible through the CAAPS GUI. Four files were produced for each model run, which contained: GRIB, METEO (graphics), OBS and CODA. NPS will manually download the bundled files for each model run.

THIS PAGE INTENTIONALLY LEFT BLANK

INITIAL DISTRIBUTION LIST

1. Defense Technical Information Center
Ft. Belvoir, Virginia
2. Dudley Knox Library
Naval Postgraduate School
Monterey, California
3. LtCol Karl Pfeiffer
Naval Postgraduate School
Monterey, California
4. Dr. Ken Davidson
Naval Postgraduate School
Monterey, California
5. Mr. Jim Ehlert
Naval Postgraduate School
Monterey, California
6. Mr. Ed Fisher
Naval Postgraduate School
Monterey, California
8. Ms. Rita Painter
Naval Postgraduate School
Monterey, California